Food Chemistry: X 20 (2023) 100935

Contents lists available at ScienceDirect

Food Chemistry: X

journal homepage: www.sciencedirect.com/journal/food-chemistry-x

Dehydration–rehydration vegetables: Evaluation and future challenges

Bixiang Wang [a], Yuanlong Jia [a], Yue Li [a], Zhitong Wang [a], Liankui Wen [a,*], Yang He [a,*], Xiuying Xu [a,b,*]

[a] Department of Food Science and Engineering, Jilin Agricultural University, Changchun 130118, China
[b] National Engineering Research Center for Wheat and Corn Deep Processing, Changchun 130118, China

ARTICLE INFO

Keywords:
Vegetables
Dehydration
Rehydration
Water migration
Quality
Rehydration model

ABSTRACT

In this review, the rehydration kinetics model, the quality factors affecting of vegetables during rehydration process, the future challenges and development direction of rehydration process were comprehensively analyzed. Based on the fitting equation for the change in moisture content during rehydration, a suitable rehydration model can be selected to describe the rehydration process of vegetables. Optimal pre-treatment, drying and rehydration methods were selected by considering quality, energy consumption and environmental aspects, and new technologies were developed to improve the quality characteristics of rehydrated vegetables. It is necessary to classify vegetables according to their shape and type to establish the criteria of rehydration processing through mathematical modeling. Industrial production from pre-treatment to product packaging will be precisely adjusted through process parameters. Furthermore, improvements the quality of rehydrated vegetables can be considered in terms of the structural and compositional aspects of the cell wall and cell membrane.

1. Introduction

Vegetables are rich in nutrients, including vitamins, minerals, trace elements and amino acids needed by the human body. At a global scale, Asia ranks first in average vegetable production from 2015 to 2020 (Fig. 1AC) (FAO, 2022a), and China ranks first in the world with 168 million tons of vegetables production (Fig. 1B). The wastage rate of fresh vegetables in developing countries is as high as 30% to 40%, therefore, it is necessary to increase the preservation rate of vegetables to improve the shelf life and economic efficiency (Bassey, Cheng, & Sun, 2021). Drying technology is an important process to solve this problem. Dehydrated vegetables can cut down on weight, make it easier to transport, extend shelf life, and have special flavor (Li, Wang, Lv, & Zhao, 2022). The volume of import and export of dehydrated vegetables from 2015 to 2020 is shown in the Fig. 1D (FAO, 2022b). The production of vegetables is substantial, with the total volume of dehydrated vegetables exported reaching 270,494 tons in 2020. Moreover, there are many different kinds of dehydrated vegetables are distributed in China, including dehydrated *Osmunda japonica*, dehydrated plum cabbage, bamboo shoots, the mushrooms, the Hericium Erinaceus, the yellow cauliflower, eggplant, potatoes, radish, and dehydrated fenugreek (Shen et al., 2018).

Most of dehydrated vegetables need to be rehydrated before consumption (Zhou et al., 2021), and the degree of recovery to the original fresh state after rehydration (restorability) is an important indicator to evaluate the quality of dehydrated vegetables. The rehydration process can be described by rehydration kinetics (Biswas, Hossain, & Zzaman, 2022). Due to the importance of dehydration–rehydration in the food industry, dehydration–rehydration dynamic models were proposed before the 1970s (Henderson, 1974), and this type of research has been conducted for decades (Labuza, 2007; Mujumdar & Erdesz, 2007; Duckworth, 1975), including theoretical and empirical models (Solomon & Jindal, 2017; Biswas, et al., 2022; Rojas & Augusto, 2018b). We summarized the important scientific contributions in studies on dehydration–rehydration (Table 1). Researchers are constantly exploring and updating to apply this model to the drying optimization process, but they still need to deepen their knowledge in this field. There is no comprehensive report on the comprehensive analysis of rehydration dynamic model, the practical use of vegetable drying and the guiding relationship between production.

The degree of rehydration indicates the degree of damage caused to the cellular structure of the dehydrated material after different treatments (Górnicki, Choińska, & Kaleta, 2020). Treatments such as pre-treatment, drying methods, and rehydration conditions can affect the restorability of dehydrated vegetables by altering their tissue structure, which then affect the mechanical support and water retention of

* Corresponding authors at: 2888, Xincheng Street, Changchun, Jilin Province 130118, China.
E-mail addresses: wenliankui@163.com (L. Wen), heyang200704@jlau.edu.cn (Y. He), xuxiuying3288@163.com (X. Xu).

https://doi.org/10.1016/j.fochx.2023.100935
Received 19 May 2023; Received in revised form 19 September 2023; Accepted 8 October 2023
Available online 12 October 2023

vegetables (Khan, Farrell, Nagy, & Karim, 2018). Research on vegetable drying mainly focuses on the development of drying methods and drying techniques, while there are fewer studies based on vegetable characteristics, pre-treatment, and rehydration methods combined with kinetic modeling to improve the restorability. The development of rehydration methods and rehydration equipment needs to be reconsidered. Furthermore, some new technologies have been found in this research process. For example, the detection of vegetable quality after rehydration includes microstructure observation and water migration. Moreover, in the recent studies, confocal Raman microscopy (CRM) imaging has been used to determine the distribution of water content at the cellular level as well as the water status of different hydrogens (Li, Zhu, & Sun, 2020). This technology has not yet been applied in rehydration studies, and future applications of this technology are also analyzed in this paper. Our review highlights for the first time the quality characteristics of rehydrated samples and the factors that characterize the product quality after rehydration. And we have sorted out and summarized the factors affecting the quality of rehydration processed vegetables, contemplated the guidance of rehydration kinetics for production and application, summarized the existing knowledge and current status as well as the latest advances, and proposed the future research directions.

2. Rehydration dynamics

2.1. Rehydration indicators

Rehydration indicators include rehydration ratio (RR), recovery factor (RF) and the average rehydration rate (AR), etc. RR is the ratio of rehydrated weight (Rw) to dehydrated weigh (Dw) (Eq. (1)). (Alolga et al., 2021; Aravindakshan, Kyomugasho, Buvé, & van Loey, 2021; Wang et al., 2019). The ratio of the Rw and the corresponding fresh weight (Fw) (Eq. (2)) is known as RF. AR is the ratio of the RR to the rehydration interval time (Δt) (Eq. (3)).

$$\mathrm{RR} = \frac{\mathrm{Rw}}{\mathrm{Dw}} \tag{1}$$

$$\mathrm{RF} = \frac{\mathrm{Rw}}{\mathrm{Fw}} \tag{2}$$

$$AR = \frac{\Delta RR}{\Delta t} \tag{3}$$

Wang, Xu, Wei, and Zeng (2018) performed low-frequency ultrasound pre-treatment on carrots and found that the ultrasound power at an input power of 1080 W results in a maximum RR (about 5.3), which is significantly higher than that without pre-treatment (about 4.2). Xu et al. (2020) demonstrated that the RR of microwave-vacuum drying (MVD) and vacuum freeze-drying (VFD) cabbages are significantly higher than that of VFD and hot air drying (HAD) (Table 1). This is due to the fact that the FD-dried Chinese cabbage product with a homogeneous honeycomb appearance and almost no collapsed structure, indicating that FD has a positive effect on the preservation of porous cell structure. MVD-dried product shows a clearer and looser porous structure than HAD and VD, which may be due to some swelling of tissue cells during microvessel densification. This would help to enhance the water absorption during rehydration, and thus reducing shrinkage.

2.2. Rehydration equations

To improve the quality of rehydration products and save energy, it is necessary to fully understand the rehydration process and optimize the rehydration conditions. Therefore, dynamic models describing water transfer are essential and the main rehydration models are Fick diffusion law, Peleg model and Weibull model (Table S1) (Benseddik, Azzi, Zidoune, Khanniche, & Besombes, 2019; Tepe & Tepe, 2020; Lopez-Quiroga, Prosapio, Fryer, Norton, & Bakalis, 2019), which can describe the rehydration process and predict the equilibrium water content. Some suitable rehydration models and rehydration parameters for vegetables under different drying methods are summarized in the

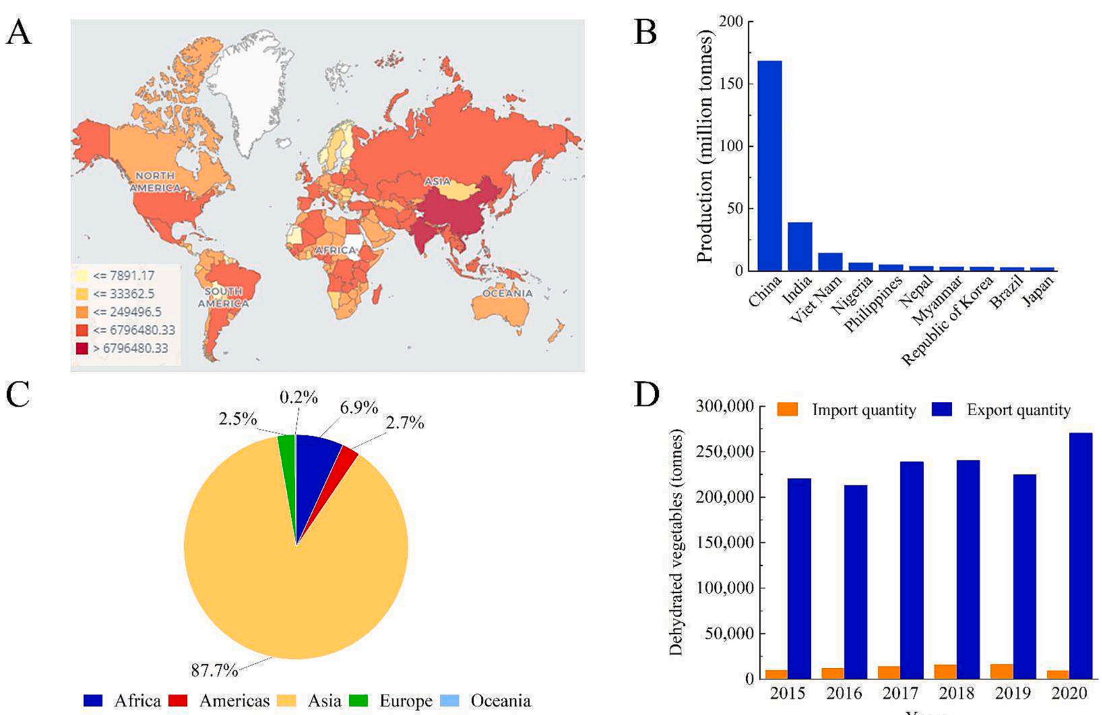

Fig. 1. The distribution of vegetables production all over the world and the trade of dehydrated vegetables in China (average 2015 ~ 2020). A: Production of fresh vegetables (updated from FAO, 2022a). B: Top 10 producers of fresh vegetables production (updated from FAO, 2022a). C: Production share of fresh vegetables by different regions (updated from FAO, 2022a). D: Dehydrated vegetable import and export volume in 2015 ~ 2020 (updated from FAO, 2022b).

Table 1
Schedule of contributions to the study of dehydration–rehydration.

Major contributor	Time	Event	Description	References
Brunauer	1938	Bet isotherm	Equation: $\frac{A_w}{(1\text{-}A_w)m} = \frac{1}{m_0c} + \frac{(c\text{-}1)A_w}{m_0c}$	Brunauer, Emmett, & Teller, 1938
Harkins	1944	Harkins jura isotherm	Equation: $\ln A_w = b - am^{-2}$	Harkins & Jura, 1944
Page	1949	Page	Equation: $MR = \exp(-kt^n)$	Page, 1949
Hukill	1954	Dehydration kinetics: Logarithmic model	Equation: $MR = a\exp(-kt) + bc$	Hukill, 1954
Scott	1957	Aw	Equation: $A_w = \frac{P_{H_2O}}{P_0} = \frac{\%RH}{100}$	Scott, 1957
Henderson and Pabis	1961	Dehydration kinetics: Henderson model	Equation: $MR = a\exp(-kt)$	Henderson & Pabis, 1961
Warner	1962	Hydrophilic Interactions	The terminology was introduced assuming the meaning of protection such that certain sugar and sugar-like molecules are provided to biological systems to prevent damage from freezing or dehydration	Warner, 1962
Thomson	1968	Dehydration kinetics: Thomson model	Equation: $t = a\ln(MR) + b\ln(MR)^2$	Thomson, Peart, & Foster, 1968
Henderson	1974	Dehydration kinetics: Two-term model	Equation: $MR = a\exp(-k_0t) + b\exp(-k_1t)$	Henderson, 1974
Henderson	1974	Dehydration kinetics: Two-term exponential model	Equation: $MR = a\exp(-kt) + (1\text{-}a)\exp(-kat)$	Henderson, 1974; Rahman, Perera, & Theband, 1998
Crank	1975	Rehydration kinetics: Fick's second law	Equation: $W_t = W_e + (W_0 - W_e)\frac{8}{\pi^2}\exp\left[\frac{-D_e\pi^2t}{4L^2}\right]$	Crank, 1975
Bruce	1985	Dehydration kinetics: Lewis model	Equation: $MR = \exp(-kt)$	Bruce, 1985
Peleg	1988	Rehydration kinetics: Peleg model	Equation: $W_t = W_0 + \frac{t}{k_1 + k_2t}$	Peleg, 1988
Machado	1998	Rehydration kinetics: Weibull model	Equation: $W_t = We + (Wo - We)\exp(-(\frac{t}{b})^a)$	Machado, Oliveira, Gekas, & Singh, 1998

Note: m, moisture content at given; Aw, water activity; P_{H2O}, the equilibrium vapor pressure that the water in a food exerts; Po, vapor pressure of pure water; % RH, relative humidity of air; mo, monolayer value; a, b, c, k, k0, k1 and k2 are constants; t, time; MR, moisture ratio; W0, initial moisture content; Wt, Water content at time t; We, equilibrium moisture content.

table for further study (Table S1), and the rehydration activation energy is derived based on different rehydration temperatures.

2.2.1. Fick diffusion law

Fick diffusion law applies to infinite flat objects with constant water diffusion coefficient (Tepe & Tepe, 2020). The rehydration kinetics are assumed to be controlled by the simplest transport of water from the surface to the center of the earth, with isotropic uniform diffusion and constant diffusivity values. It is also assumed that the dimensions of the substrate remain at a constant value during rehydration process. It is affected by the gradual instability and has an initial uniform distribution and equal concentration on the surface. It is assumed that the passing matrix is an infinite plate with uniform (negligible shrinkage or expansion) initial humidity distribution, negligible external resistance and constant diffusivity coefficient (Benseddik et al., 2019).

As a typical theoretical model, Fick's diffusion law (Eq. (4)) can describe the mass transfer process. Fick's second law is used to estimate the effective diffusion coefficient, (Deff) in the rehydration process, which is a dynamic process involving multiple parameters, so it is inconvenient to calculate in most cases (Benseddik et al., 2019).

$$Wt = We + (Wo - We)\frac{8}{\pi^2}\exp\left[\frac{-Deff\pi^2t}{4L^2}\right] \tag{4}$$

Wt is the moisture content [g water/g dry matter (d.m.)] at time t (min), We is the equilibrium moisture content (g water/g d.m.), Wo is the initial moisture content (g water/g d.m.), Deff is the effective diffusion coefficient (m^2/s), t is the rehydration time (min), and L is the half-thickness slice (m). De generally increases with increasing rehydration temperature, indicating that rehydration is favored by appropriately high temperatures (Zura-Bravo, Ah-Hen, Vega-Gálvez, García-Segovia, & Lemus-Mondaca, 2013). The conditions of this equation are based on the following assumptions: uniform initial moisture distribution, constant effective diffusion coefficient, and no shrinkage.

2.2.2. Peleg model

A two-parameter non-exponential equation was proposed by Peleg in 1988, which is a non-theoretical non-diffusion model, but an empirical model (Tepe & Tepe, 2020). This model has been applied to describe the rehydration process of various food products. The equation is relatively easy to calculate. The greatest advantage of model is that short-term rehydration data can be used to predict the equilibrium moisture content of vegetables. The equation (Eq. (5)) is as follows:

$$Wt = Wo + \frac{t}{k_1 + k_2t} \tag{5}$$

k_1 is a constant related to the mass transfer rate [min (kg d.m.) (kg water)$^{-1}$], and it is found that the lower value of k_1 means the higher the initial water rehydration rate. When $t \to \infty$, the equilibrium water content will be obtained by the following equation (Eq. (6)).

$$Wt = Wo + \frac{1}{k_2} \tag{6}$$

k_2 is the capacity constant [(kg d.m.) (kg water)$^{-1}$] of Peleg, which is related to the maximum water absorption. The value of k_2 depends on the type, structure and chemical composition of the material and may be modified by heat treatment. If a temperature change during rehydration induces a change of tissue structure or other properties, which in turn changes the k_2 value. General speaking, a certain temperature range, the higher the temperature, the lower k_2 value and the higher water absorption rate during rehydration process (Lopez-Quiroga, Prosapio, Fryer, Norton, & Bakalis, 2019).

2.2.3. Weibull model

The Weibull model is an empirical model widely used in food engineering. Because of the simplicity and flexibility of estimating parameters, it is widely used in food engineering, and the rehydration processes of most vegetables accords with this model (Eq. (7)) (Ansari, Maftoonazad, Farahnaki, Hosseini, & Asadi, 2015).

$$Wt = \mathrm{We} + (\mathrm{Wo} - \mathrm{We})\exp(-(\frac{t}{\beta})^{\alpha}) \quad (7)$$

α is a dimensionless shape parameter, which indicates the water absorption rate at the beginning of rehydration. The lower the value, the faster the water absorption rate begins (Uribe et al., 2011). Different α values can represent different curves, which can describe different rehydration mechanisms (including diffusion, convection and relaxation). β is a rate parameter, defined as the rate of moisture absorption process, which represents the time required to complete about 63% rehydration process (Demirhan & Özbek, 2010).

The Arrhenius equation (Eq. (8)) can be used to calculate the activation energy in the rehydration process (Maneesh, Prasad, Chandra, & Debnath, 2018).

$$\Phi = \Phi_0 \exp\left[-\frac{E_a}{\mathrm{RT}}\right] \quad (8)$$

Φ is the kinetic parameter of each model (De, k_1, k_2, A, and B), Φ_0 is the coefficient of the Arrhenius equation, Ea is the activation energy, R is the ideal gas constant (8.314 J mol^{-1} K^{-1}), T is the absolute value of temperature in the rehydration process (K).

For the selection of each rehydration model, each rehydration model can be fitted according to the migration of rehydration time during rehydration process and the water content of the sample, so as to select a model suitable for each vegetable rehydration. Demiray and Tulek (2017) found that the values of parameters k_1 and k_2 in the Peleg model of red pepper showed a decreasing trend as the temperature increased from 25 °C to 45 °C, indicating that the rehydration process accelerated with the increase of rehydration temperature. According to the reported studies, the Ea required for rehydration of apple slices at 20–60 °C was reported to be 11.29 kJ/mol (Fick model) and De increased with the increasing temperature (from 1.36×10^{-9} to 2.37×10^{-9} m^2/s) (Zura-Bravo, Ah-Hen, Vega-Gálvez, García-Segovia, & Lemus-Mondaca, 2013).

3. Influence factors of rehydration

3.1. Vegetable characteristics

Vegetable characteristics, such as vegetable type, size, freshness, production location, varieties of same vegetable, etc., have an important effect on the restorability of dried vegetables. Previous studies have found that different varieties have different rehydration abilities. Three dried tomatoes (cultivars 18131, 18146, and 1862) were rehydrated, and found that the 18,131 variety exhibited a higher rehydration capacity than other two cultivars in both OD and FD samples (Tan et al., 2021). The authors did not analyze the differences in rehydration caused by different varieties, but we hypothesize that since different varieties of tomatoes contain different nutrients and chemical compositions, there are differences in the structure of the dried tomatoes leading to differences in rehydration. Similarly, Markowski et al. (2006) conducted on the rehydration characteristics of six carrot varieties and found that the rehydration process was influenced by carrot varieties. The authors believe that the change of different varieties after rehydration may be the difference of chemical composition, including the binding ability of protein. Proteins are associated with fiber binding, film formation, and also viscosity, which has an effect on water retention and adsorption. Furthermore, the maturity level of vegetables can also impact both the drying and rehydration processes. Li et al. (2022) analyzed the far infrared drying kinetics of mangoes at different stage of ripening. The four stages from the lowest to the highest ripeness are referred to as RS-1, RS-2, RS-3 and RS-4, respectively. The results showed that maturity RS-3 had the shortest drying time and the largest diffusion coefficient. This variation could be attributed to differences in maturity, cell wall degradation, and accelerated water outflow. The cell wall structure was disrupted as the fruit matured, the molecular weight of pectin decreased, pectin dissolved and depolymerized, and the hemicellulose content showed an overall decreasing trend, thus disrupting the arrangement of the cell wall. This phenomenon hinder water migration during drying and reduce the drying rate. Unfortunately, the authors did not perform rehydration analyses, but based on the changes in drying, it is reasonable to hypothesize that structural changes are responsible for rehydration. The group's previous studies (Wang et al., 2023) have shown that changes in the cell wall and cell membrane of the samples do affect the dehydration-rehydration process. In the future, we need to continue to study and verify our speculations in this regard applying some techniques (Including detection of structural and moisture changes such as CRM). This is meaningful for the production of special-purpose foods.

3.2. The effect of pre-treatments on rehydration

3.2.1. Effect of cutting pre-treatment on rehydration

Methods of cutting vegetables include transversal cutting, longitudinal cutting, and punching, etc. The difference in cutting methods affect the variation of rehydration rate. Rojas and Augusto (2018c) documented a higher rehydration rate after longitudinal (Lc) cutting than transversal cutting (Tc) of pumpkin. However, the rehydration rate of Tc exceeds that of Lc when the rehydration time exceeds 180 min, (Fig. 2A). In the rehydration process of Lc sample, water enters quickly through the xylem catheter, which is due to the length and orientation of the xylem catheter, resulting in a higher rehydration rate (Khan, Nagy, & Karim, 2018). Hence, the rehydration mechanism is found to be mainly water transfer through capillary action in the xylem. Currently, in order to avoid the problem of nutrient loss in the Lc and Tc, mechanical perforations were being investigated to increase the drying rate and rehydration capacity (Rojas, Silveira, & Augusto, 2019). The intricate tissue structure of the food impedes water flow, while the perforations facilitate water absorption via capillary action. Certainly, the size and density of the perforations play a significant role in the rehydration process, which is an important consideration.

3.2.2. Effect of blanching pre-treatment on rehydration

Hot blanching is usually carried out under high temperature and normal pressure (usually ranging from 75 °C to 95 °C), with a blanching time between 1 and 10 min. Blanching treatment excludes air from vegetable tissues, removes some water from the tissues, and increase cell permeability and tissue softening (Deng et al., 2019; Wang et al., 2021), which helps to accelerate the RR.

Blanching is a common hot water bath treatment (Tao et al., 2019). High-humidity hot air impingement blanching (HHAIB) is a high-speed, high-efficiency thermal treatment technology developed in recent years (Zhou et al., 2022). The blanching time of HHAIB is related to the RR. According to Wang et al. (2023), HHAIB treatments of red pepper for different durations (0, 30, 60, 90, 120 and 150 s) revealed that the RR of 90 s hot blanching pre-treatment (about 2.4) was significantly higher than that of other treated samples (Table 2). After HHAIB treatment, the microstructure was disrupted to varying degrees. And after 90 s of treatment, the intermediate layer was dissolved, the cytoplasmic membrane was disrupted, and the RR value after drying was the largest, which could be attributed to the disruption of the cellular structure, the porosity of the samples was bigger, and the rehydration ability was stronger. During hot blanching, vegetable tissues undergo profound cellular structural changes, which can enhance mass transfer and promote water transfer in the tissues (Deng et al., 2018, 2019; Wang et al., 2017), however, the mechanism of accelerated mass transfer by blanching has not been thoroughly studied. Moreover, the temperature and duration of the blanching treatment should be strictly controlled according to the specific characteristics of the vegetables.

In recent years, researchers have discovered the non-thermal blanching, high hydrostatic pressure (HHP) blanching, with pressure

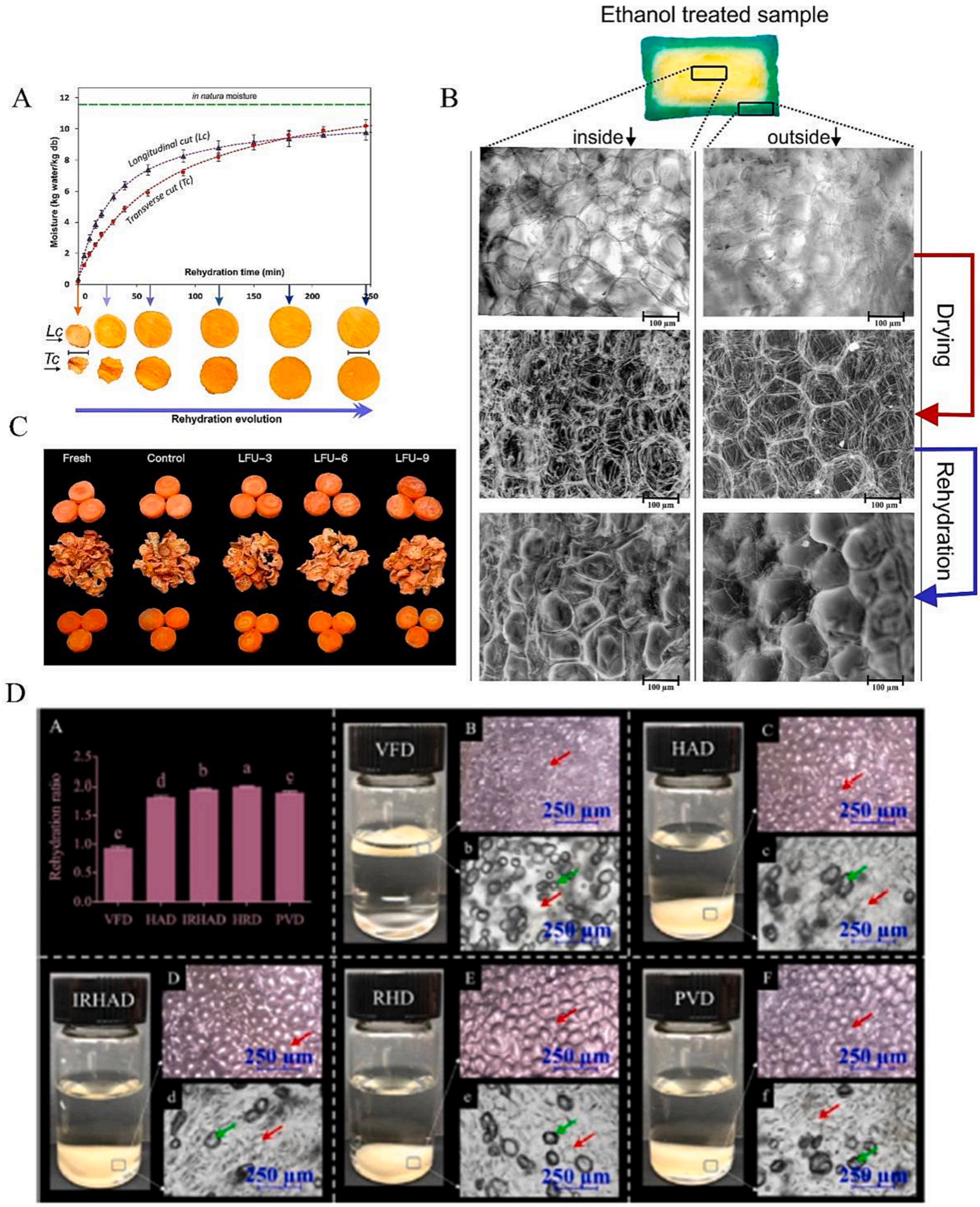

Fig. 2. Effects of cutting and osmotic pre-treatments and drying methods on vegetables rehydration. A: The impact of cutting pre-treatment on rehydration of pumpkin. The figures were reproduced from Rojas and Augusto (2018c) with the permission from Elsevier. B: Ethanol treatment on the structure of pumpkin structure after rehydration. The figures were reproduced from Rojas and Augusto (2018b) with the permission from Elsevier. C: The effect of low-frequency ultrasound pre-treatment on carrots after rehydration. The figures were reproduced from Wang et al. (2018) with the permission from Elsevier. D: The effects of different drying methods on the garlic after rehydration. The figures were reproduced from Feng et al. (2021) with the permission from Elsevier.

usually as 100 MPa or higher, which can make the product microorganisms and enzymes are greatly reduced. Vegetable samples obtained by HHP have good color and less nutrients loss, making it a favorable alternative to traditional hot blanching. Moreover, HHP has been widely used for the pre-treatment before drying to shorten the drying time (Zhang et al., 2020). However, it has not been widely used in the rehydration processing of vegetables. Most importantly, HHP has been less studied on rehydration vegetables, whether it helps to rehydration is unknown, and more researches could be done in the future.

3.2.3. *Effect of osmotic dehydration pre-treatment on rehydration*

Osmotic dehydration is now considered as a valuable technique for minimal food processing (Sakooei-Vayghan, Peighambardoust, Hesari, & Peressini, 2020; Osae et al., 2020a). Commonly used osmotic substances include ethanol, sugar and certain salts. Osmosis is the process of utilizing osmotic pressure to transfer water from tissues through a semipermeable membrane into an osmotic solution, while simultaneously allowing solutes from the osmotic solution to be absorbed into tissues (Bozkir, Ergün, Serdar, Metin, & Baysal, 2019; Rahaman et al., 2019). The osmotic substances into the vegetables, allowing more hydrophilic substances to be stored in the tissue voids. And the samples are

Table 2
The impact of different treatment on the rehydration ratio of dehydrated vegetables.

Species	Pre-treatments methods	Pre-treatments conditions	Drying methods	Drying conditions	Water activity	Rehydration temperature (°C)	Rehydration time (h)	RR/(%)/(d.b.)	References
Cabbage	Blanching	100 °C, 30 s	HAD	60 °C	–	25	–	~7.1	(Tao et al., 2019)
Cabbage	Blanching	30 s	US + HAD	60 °C, 492.3 W/m^2, 2 h	–	25	–	7.75	(Tao et al., 2019)
Cabbage	Blanching	30 s	US + HAD	60 °C, 1131.1 W/m^2, 1.75 h	–	25	–	~7.3	(Tao et al., 2019)
Cabbage	–	–	US + HAD	60 °C, 492.3 W/m^2, 2 h	–	25	–	~7.15	(Tao et al., 2019)
Cabbage	–	–	US + HAD	60 °C, 1131.1 W/m^2, 1.75 h	–	25	–	~7.25	(Tao et al., 2019)
Cabbage	–	–	HAD	60 °C	–	25	–	~7.07	(Tao et al., 2019)
Red pepper	HHAIB	110 °C, 35–40% humidity, 30 s	HAID	65 °C, 14.0 ± 0.5 m/s	–	60	2	~2.0	(Wang et al., 2023)
Red pepper	HHAIB	110 °C, 35–40% humidity, 60 s	HAID	65 °C, 14.0 ± 0.5 m/s	–	60	2	~2.1	(Wang et al., 2023)
Red pepper	HHAIB	110 °C, 35–40% humidity, 90 s	HAID	14.0 ± 0.5 m/s, 65 °C	–	60	2	~2.5	(Wang et al., 2023)
Red pepper	HHAIB	110 °C, 35–40% humidity, 120 s	HAID	14.0 ± 0.5 m/s, 65 °C	–	60	2	~2.3	(Wang et al., 2023)
Red pepper	HHAIB	110 °C, 35–40% humidity, 150 s	HAID	14.0 ± 0.5 m/s, 65 °C	–	60	2	~2.4	(Wang et al., 2023)
Carrot	Ethanol + US	25 kHz, 20 °C, 99.8% ethanol (v/v), 30 min	HAD	–	–	25 ± 1	8	~85%	(Santos et al., 2021)
Carrot	Ethanol	99.8% (v/v) for 30 min	HAD	–	–	25 ± 1	8	~81%	(Santos et al., 2021)
Carrot	Water + US	25 kHz at 20 °C, water, 30 min	HAD	–	–	25 ± 1	8	~55%	(Santos et al., 2021)
Carrot	US + OD	25 kHz, 20 ± 1 °C, 99.8% (v/v) ethanol, 30 min	HAD	40 °C, 4 h	–	25	8	~85%	(Santos et al., 2021)
Pumpkin	–	–	HAD	60 °C, 16.33 h	0.438 ± 0.021	25 80	–	3.138 ± 0.456 3.968 ± 0.140	(Monteiro et al., 2018)
Persimmon	10 US + OD	45 °Brix sucrose solution, US for 10 min, 35 kHz	HAD	60 °C, 1.5 m/s	–	50	0.83	1.764 ± 0.032	(Bozkir et al., 2019)
Persimmon	20 US + OD	45 °Brix sucrose solution, US for 20 min, 35 kHz	HAD	60 °C, 1.5 m/s	–	50	0.83	1.949 ± 0.021	(Bozkir et al., 2019)
Persimmon	30 US + OD	45 °Brix sucrose solution, US for 20 min, 35 kHz	HAD	60 °C, 1.5 m/s	–	50	0.83	1.875 ± 0.044	(Bozkir et al., 2019)
Persimmon	–	–	HAD	60 °C, 1.8 m/s, 7 h	–	80	0.4	1.833 ± 0.023	(Bozkir & Ergün, 2020)
Tomato	DW	–	HAD	55 °C, 1.5 m/s	–	25	–	~2.6	(Obajemihi et al., 2023)
Tomato	PW	–	HAD	55 °C, 1.5 m/s	–	25	–	2.89	(Obajemihi et al., 2023)
Tomato	OD	25.8 °C, 40% sucrose solution	HAD	55 °C, 1.5 m/s	–	25	–	1.89	(Obajemihi et al., 2023)
Tomato	PO	–	HAD	55 °C, 1.5 m/s	–	25	–	~2.0	(Obajemihi et al., 2023)
Tomato	–	–	HAD	70 °C, 12 h.	–	Room temperature	12	3.67 ± 0.05	(Tan et al., 2021)
Tomato	–	–	VFD	Frozen at −80 °C for 12 h, dried for 48 h	–	Room temperature	12	3.83 ± 0.21	(Tan et al., 2021)
Mushroom	–	–	HAD	45 °C, 60 °C, 9 h	–	60	–	~420%	(Xu et al., 2019)
Mushroom	–	–	HAD	55 °C, 60 °C, 9 h	–	60	–	~442%	(Xu et al., 2019)
Mushroom	–	–	HAD	55 °C, 60 °C, 9 h	–	60	–	~445%	(Xu et al., 2019)
Mushroom	–	–	HAD	75 °C, 60 °C, 9 h	–	60	–	452.97%	(Xu et al., 2019)
Mushroom	–	–	HAD	60 °C, 2 m/s, 13.5 h	0.35 ± 0.00	40	3.33	4.64 ± 0.32	(Zhao et al., 2019)

(continued on next page)

Table 2 (*continued*)

Species	Pre-treatments methods	Pre-treatments conditions	Drying methods	Drying conditions	Water activity	Rehydration temperature (°C)	Rehydration time (h)	RR/(%)/(d.b.)	References
Cabbage	–	–	HAD	60 °C, 3 m/s, 8.5 ± 0.5 h	–	80	0.25	~7	(Xu et al., 2020)
Mushroom	–	–	FIRD	60 °C, 2 m/s, 1350 W, 5.8 ~ 6.2 μm (wavelength), 10.5 h, 0.056 g/g/min	0.27 ± 0.00	40	3.33	7.31 ± 1.72	(Zhao et al., 2019)
Pumpkin	–	–	MWVD	1000 W, 300 W, 200 W, 3 ~ 5 kPa, 1.28 h	0.342 ± 0.049	25	–	15.307 ± 0.580	(Monteiro et al., 2018)
Pumpkin	–	–	MWVD	1000 W, 300 W, 200 W, 3 ~ 5 kPa, 1.28 h	0.342 ± 0.049	80	–	7.176 ± 0.263	(Monteiro et al., 2018)
Pumpkin	–	–	KMFD	60 °C, 90 °C, 3 ~ 5 kPa, 3.50 h	0.385 ± 0.010	25	–	5.781 ± 0.320	(Monteiro et al., 2018)
Pumpkin	–	–	KMFD	60 °C, 90 °C, 3 ~ 5 kPa, 3.50 h	0.385 ± 0.010	80	–	6.117 ± 0.125	(Monteiro et al., 2018)
Pumpkin	–	–	HAD + DIC + HAD	60 °C, 1.2 m/s, 5 KPa, 0.40 MPa, 5 KPa (DIC cycle), 0.08 h	–	–	–	0.98	(Benseddik et al., 2019)
Pumpkin	–	–	VMFD	60 °C, 300 KPa, 100 KPa (cycles), 0.42 h	–	–	–	0.98	(Benseddik et al., 2019)
Cabbage	–	–	MWVD	6 W/g, 1.1 ± 0.5 h	–	80	0.25	~7.5	(Xu et al., 2020)
Cabbage	–	–	VD	60 °C, 100 Pa, 7.5 ± 0.6 h	–	80	0.25	~7.1	(Xu et al., 2020)
Cabbage	–	–	MD+ VD	60 °C, 6 W/g, 100 Pa, 3.4 ± 0.6 h	–	80	0.25	~7.1	(Xu et al., 2020)
Cabbage	–	–	MD + HAD	6 W/g, 60 °C, 3.0 m/s, 3.6 ± 0.4 h	–	80	0.25	~7.2	(Xu et al., 2020)
Chinese ginger	DW	–	IRD	60 ± 2 °C	–	30 ± 1	–	4.81 ± 0.38	(Ren et al., 2022)
Potato	DW	–	IRD	100 °C, 95% IR radiation	–	24 ± 1	6.33	78.3%	(Rojas & Augusto, 2018a)
Chinese ginger	Water + US	40 kHz, 300 W, 25 ± 1 °C for 15 min	IRD	60 ± 2 °C	–	30 ± 1	–	3.87 ± 0.28	(Ren et al., 2022)
Potato	Water + US	40 kHz, 300 W, 25 ± 1 °C for 15 min	IRD	100 °C, 95% IR radiation	–	24 ± 1	6.33	77.7%	(Rojas & Augusto, 2018a)
Chinese ginger	Ethanol	75 % ethanol solution (v/v)	IRD	60 ± 2 °C	–	30 ± 1	–	5.07 ± 0.30	(Ren et al., 2022)
Potato	Ethanol	–	IRD	100 °C, 95% IR radiation	–		6.33	76%	(Rojas & Augusto, 2018a)
Scallion	DW	25 ± 1 °C,	IRHAD	225 W, 60 ± 2 °C, 2 m/s.	–	25	0.43	~4.5	(Wang et al., 2019)
Scallion	Ethanol	25 ± 1 °C, 75% ethanol solution at a ratio of 1:8 (w/w).	IRHAD	225 W, 60 ± 2 °C, 2 m/s.	–	25	0.43	~5.3	(Wang et al., 2019)
Scallion	Vacuum + Water + VC	25 ± 1 °C, 0.6 bar vacuum	IRHAD	225 W, 60 ± 2 °C, 2 m/s.	–	25	0.43	~4.9	(Wang et al., 2019)
Scallion	Vacuum + Ethanol + VC	25 ± 1 °C,75% ethanol solution at a ratio of 1:8 (w/w), 0.6 bar vacuum	IRHAD	225 W, 60 ± 2 °C, 2 m/s.	–	25	0.43	~5.8	(Wang et al., 2019)
Chinese ginger	Ethanol + US	150 mL of 75 % ethanol solution (v/v), 40 kHz, 300 W, 25 ± 1 °C for 15 min	IRD	60 ± 2 °C	–	30 ± 1	–	3.02 ± 0.06	(Ren et al., 2022)
Potato	Ethanol + US	–	IRD	100 °C, 95% IR radiation	–	–	6.33	74.6%	(Rojas & Augusto, 2018a)
Carrot	–	–	VD + PEF	1.5 kV, 10 ~ 1000 μs, 3.03 × 104 Pa 25 °C, 3 h	–	25	2.5	0.76	(Liu et al., 2020)
Carrot	–	–	VD + PEF	1.5 kV, 10 ~ 1000 μs, 3.03 × 104 Pa 25 °C, 1 h	–	25	2.5	0.89	(Liu et al., 2020)
Garlic	OD	$CaCl_2$ of concentration 30% (w/v)	US + OD + RHCD	40 kHz, 600 W, 30 °C, 60 °C, 2 m/s, 5.16 h	–	25	1	9 ~ 10	(Alolga et al., 2021)
Garlic	OD	$CaCl_2$ of concentration 30% (w/v)	V + US + OD + RHCD	100 mbar, 40 kHz, 600 W, 30 °C, 60 °C, 2 m/s, 4.33 h	–	25	1	11 ~ 12	(Alolga et al., 2021)

(continued on next page)

Table 2 (*continued*)

Species	Pre-treatments methods	Pre-treatments conditions	Drying methods	Drying conditions	Water activity	Rehydration temperature (°C)	Rehydration time (h)	RR/(%)/(d.b.)	References
Garlic	–	–	VFD	−40 °C, −18 °C, 0.518 mbar, 13.5 ± 0.0 h	0.3453	25	–	0.93	(Feng et al., 2021)
Cabbage	–	–	VFD	−40 °C, 60 Pa, 24.0 ± 1.4 h	–	80	0.25	~7.8	(Xu et al., 2020)
Garlic	–	–	IRHAD	60 °C, 2 m/s, 350 W, 2.8 ~ 3.1 μm, 3.8 ± 0.3 h	0.3394 ~ 0.3453	25	–	~2.0	(Feng et al., 2021)
Garlic	–	–	PVD	0.01 MPa, 60 °C, 4.8 h	–	25	–	1.82 ~ 2.00	(Feng et al., 2021)
Garlic	–	–	RHCD	37% humidity, 60 °C, 2 m/s, 4.6 ± 0.1 h	~0.35	25	–	0.93	(Feng et al., 2021)
Lotus (Nelumbo nucifera Gaertn.) seeds	US	6.08 W/cm^2, 10 min	MVD	15 W/g, 20 kPa	–	60	3.33	~0.62 d.b.	(Zhao et al., 2021)
Lotus (Nelumbo nucifera Gaertn.) seeds	US	8.39 W/cm^2, 10 min	MVD	15 W/g, 20 kPa	–	60	3.33	~0.70 d.b.	(Zhao et al., 2021)
Lotus (Nelumbo nucifera Gaertn.) seeds	US	10.84 W/cm^2, 10 min	MVD	15 W/g, 20 kPa	–	60	3.33	~0.85 d.b.	(Zhao et al., 2021)
Edamame	–	–	HD	70 °C	0.484 ± 0.006	25	2	1.17 d.b.	(An et al., 2022)
Edamame	–	–	MRD	600 W, 30 °C	0.493 ± 0.003	25	2	1.30 d.b.	(An et al., 2022)
Edamame	–	–	HMRD	600 W, 60 °C	0.479 ± 0.004	25	2	1.23 d.b.	(An et al., 2022)
Edamame	–	–	PSMVD	≤ 2500 Pa	0.464 ± 0.004	25	2	1.50 d.b.	(An et al., 2022)
Edamame	–	–	VFD	≤ 10 Pa	0.401 ± 0.005	25	2	1.67 d.b.	(An et al., 2022)
Garlic	–	–	HAD	60 °C, 2 m/s	–	Normal rehydration: 25 Vacuum rehydration: 25	2	Normal rehydration: ~2 Vacuum rehydration: ~3.1	(Zhou et al., 2021)
Garlic	–	–	HAD	60 °C, 5.9 h	–	25	–	1.82	(Zhou et al., 2021)
Garlic	–	–	VFD	0.518 mbar vacuum, cold-trap temperature of −85 °C, 60 °C, 2 m/s	–	25 Vacuum rehydration: 25	2	Normal rehydration: ~1.7 Vacuum rehydration: ~2.9	(Zhou et al., 2021)

Note: HAD: hot air drying; VFD: vacuum freeze-drying; MD: microwave drying; IRHAD: infrared hot air drying; IRD: infrared drying; FIRD: far infrared radiation drying; MWMFD: microwave multiple flash drying; MWVD: microwave-vacuum drying; KMFD: conductive multiple flash drying; DIC: drying with instant controlled; VMFD: vacuum multiple flash drying; US: Ultrasound; VD: vacuum drying; PEF: pulsed electric fields; PVD: pulse vacuum drying; RHCD: relative humidity convective drying. HAID: Hot air impingement drying; ΔE: color difference; RR: Rehydration ratio; HHAIB: High-humidity hot air impingement blanching; EP: Electroplasmolysis; US: Ultrasound; DW: distilled water; PW: plasma functionalized water; OD: osmodehydration; PO: plasma functionalized water and osmotic dehydration; ~: represent approximate.

dehydrated and then rehydrated, facilitating easy water absorption and improving RR.

Ethanol. Ethanol used in osmotic dehydration may contribute to structural changes, which is the main factor contributing to the improvement of the rehydration process. Firstly, osmosis increases the cell permeability and makes it easier for water to enter, thus facilitates the rehydration processes. Secondly, the cytoskeleton structure was better supported after ethanol treatment, thus reducing the shrinkage during drying and improving the rehydration process (Llavata, García-Pérez, Simal, & Cárcel, 2020; Rojas, Augusto, & Cárcel, 2020). The sample exhibits a tight appearance after ethanol pre-treatment, which is due to ethanol permeation excluding some air and solutes from the sample. A clear cellular structure is observed inside the sample (Fig. 2B). After drying, the sample exhibits a wrinkled appearance, with visible parenchymal cells and shrinkage in the internal cells, accompanied by the presence of air. After rehydration, the cells in the sample exhibit significant swelling. This can be attributed to the thinner cell wall and increased permeability of the pumpkin slices through ethanol treatment, which made it easier for water to enter the interior of the samples through the cell walls, thus improving rehydration (Rojas & Augusto, 2018a). Santos et al. (2021) pre-treated carrots with ethanol + ultrasonic (US), ethanol, water + US, US + OD. The results showed that the RR of samples pre-treated with ethanol + US was the highest (~85%) after drying. This is due to the fact that ethanol treatment also mixes water well, and tissue and cellular structure changes that favor water transfer and/or retention, avoiding the negative effects of drying on rehydration. However, ethanol pre-treatment can change the color of vegetables (Feng et al., 2019). Therefore, maintaining color characteristics and controlling pre-treatment time need to be considered to ensure quality.

Sugar. Sugar (including sucrose, cyclodextrin, konjac flour, hyaluronic acid, trehalose, fungus polysaccharide) and other water-retaining substances are used in osmotic dehydration (Lech, Adam, Michalska, Wojdyło, & Nowicka, 2018). After osmotic dehydration, the rehydration capacity can be improved, resulting in a relatively uniform and flat shape with minimal shrinkage phenomenon (Nowacka et al., 2019). Osmotic dehydration samples have a higher rehydration capacity than non-osmotic samples due to the increased solids content of the tissue by the osmotic solution. (Control RR: 1.081 ± 0.016; OD: 1.949 ± 0.021) (Table 2) (Bozkir, Ergün, Serdar, Metin, & Baysal, 2019). The increase of solid content makes the sample absorb more water after rehydration, and the RR is higher. Our team carried the osmotic dehydration with crude fungus polysaccharide and purification of polysaccharide with smaller molecular, the results showed that the RR of purification after osmotic was larger due to the fact that smaller molecular weights permeate better, whereas the large molecular weight of the crude polysaccharide affects the migration of water (Su et al., 2022). High concentration of osmotic solution can form an encapsulated film on the surface of vegetables. This film hinders water discharge during drying and makes rehydration more challenging to achieve. Therefore, the type, concentration and proportion of osmotic solution are especially important during the experiment (Miano, Rojas, & Augusto, 2021). The potential application of osmotic pre-treatment for the restorability of dehydrated vegetable is great. The applications of complex osmotic solutions and different processing techniques in assisting osmotic dehydration can provide a reference for vegetables processing. Nevertheless, it is inevitable that the flavor and texture of the sample may undergo changes upon immersion in the osmotic solution. (Bozkir, Ergün, Serdar, Metin, & Baysal, 2019). The RR was found to be maximum for the samples treated with 45 °Brix sucrose solution, US for 20 min, 35 kHz (1.949 ± 0.021) (Table 2). This may be due to the fact that ultrasound accelerates the penetration of the sugar solution, maintains the structural skeleton of the sample, improves the mechanical capacity of the sample, retains water better after rehydration, and improves rehydration rate (Kumar et al., 2021). After permeation with ethanol and sugar solution most of the samples exhibit a higher RR (Table 2). However, Obajemihi, Esua, Cheng, and Sun (2023) reported that the sugar solution was applied for osmotic pre-treatment resulted in lower RR compared to samples without osmotic pretreatment. The solute enters the tissue during infiltration process and the solute retained in the tissue is immersed in the solution after rehydration, which reduces the overall mass of rehydrated sample, resulting in a reduction in the RR. Moreover, the prolonged infiltration time increases the number of microorganisms in the infiltrate, and a large amount of osmotic solution recycling and management issues require careful attention.

3.2.4. Effect of emerging pre-treatment methods on rehydration

With the high demand for the quality of dehydrated vegetables, new pre-treatment methods emerged (Zhou et al., 2020), such as cold plasma (CP) and low-frequency ultrasound. CP is used in food drying and is a non-chemical treatment that breaks down the wax layer barrier's impediment to moisture migration, thus facilitating moisture diffusion and evaporation (Zhang et al., 2019). Li et al. (2019) found that the pre-treatment with CP reduced drying times and increased drying rate. The mechanism of drying behavior and quality property changes caused by CP pre-treatment is still unclear. It is speculated that the CP treatment may destroy the cell wall and cell membrane, promote the water removal and accelerate drying rate (Liu, Pirozzi, Ferrari, Vorobiev, & Grimi, 2020). However, the effect of CP treatment on rehydration process has received limited attention and requires further investigation. Atomic force microscopy (AFM) observation revealed severe surface loss of drying samples after CP treatment (Wang et al., 2018). Studies have shown that AFM combined with image analysis can directly observe and quantitatively analyze the conformational characteristics of individual molecules, such as length, diameter, branching, chain aggregation and supramolecular assembly (Zdunek, Pieczywek, & Cybulska, 2021).

Other emerging pre-treatment methods include low-frequency ultrasound (LFU), US and pulsed electric fields (PEF). According to Wang et al. (2018), carrot slices were pretreated with LFU exhibited a higher rehydration rate during the rehydration process. The microchannels formed after US pre-treatment, which can alter the mass transfer and cell walls permeability of vegetables, resulting in improved drying and rehydration characteristics. The color parameters of dried carrot slices pretreated by US are closer to those of rehydrated carrot samples (Fig. 2C). The shorter drying time and browning time of the LFU pre-treatment samples are responsible for the better retention of the original color. Currently, pre-treatment technologies such as US waves and pulsed electric fields (PEF) can shorten the pre-treatment time by assisting osmotic substances (Osae et al., 2020b). Liu et al. (2020) reported that the dried PEF carrots were rehydrated, the samples basically recovered their original morphology and tissue structure as observed by SEM (Fig. 3A). The structure of the dried PEF carrots appeared to be more homogeneous than that of the untreated carrots, which explains the higher rehydration capacity of dried PEF samples. US pre-treatment researches has been studied for many years (Andreou, Dimopoulos, Dermesonlouoglou, & Taoukis, 2020), but the impacts of US on the water migration and rehydration process needs to be studied in depth.

3.3. Effects of drying methods on rehydration

Different drying methods (such as, HAD, VFD, microwave drying (MD), radiation drying, combined drying, etc.) (Kayacan et al., 2020; Managa, Sultanbawa, & Sivakumar, 2020; Shi et al., 2021), and drying conditions (such as temperature, air velocity, power, etc.) have different degrees of alteration on the microstructure of vegetable tissues, which mainly in cell damage, collapse, cavity formation and shrinkage. Excessive structure deformation reduces the water absorption and retention capacity, thus affecting the rehydration process and rehydration rate (Chen et al., 2020; Monteiro, Link, Tribuzi, Carciofi, & Laurindo, 2018).

3.3.1. Effects of hot air drying on rehydration

HAD is a process that diffuses the heat energy is diffused from the surface to the inside of the material, so that the temperature inside the material gradually rises and the water migrates outwards (Xu et al., 2018; Kumar et al., 2021). In the study of Qiu et al. (2021), the microstructure of rehydrated shiitake mushrooms at different drying temperatures was observed by TEM (Fig. 3C). The results indicated that drying temperatures above 60 °C led to shrinkage of hyphae in rehydrated shiitake mushrooms. Shrinkage may be caused by the loss of rigidity of cell wall due to high temperature drying. In addition, the irreversible loss of cell membrane integrity due to dehydration. The researchers rehydrated cabbage (Tao et al., 2019), pumpkin (Monteiro, et al., 2018; Benseddik, et al., 2019), tomato (Obajemihi, et al., 2023) and garlic (Zhou, et al., 2021; Feng, et al., 2021) at 25 °C after HAD and found that the maximum RR for cabbage was 7.07 (Table 2). This may be due to the variation in different types of vegetables. The high fiber content of cabbage may be responsible for the high RR, and future studies could investigate the effect of vegetable composition on RR. Low-field nuclear magnetic resonance (LF-NMR) is used to analyze the physicochemical properties of samples by relaxation signals (Fan & Zhang, 2019). Qiu et al. (2021) investigated the moisture changes of shiitake mushrooms after rehydration at various drying temperatures using LF-NMR and magnetic resonance imaging (MRI) (Fig. 3E), which showed that shrinkage induced by high temperature drying caused the pore spaces to collapse, resulting in a decrease in the water content of

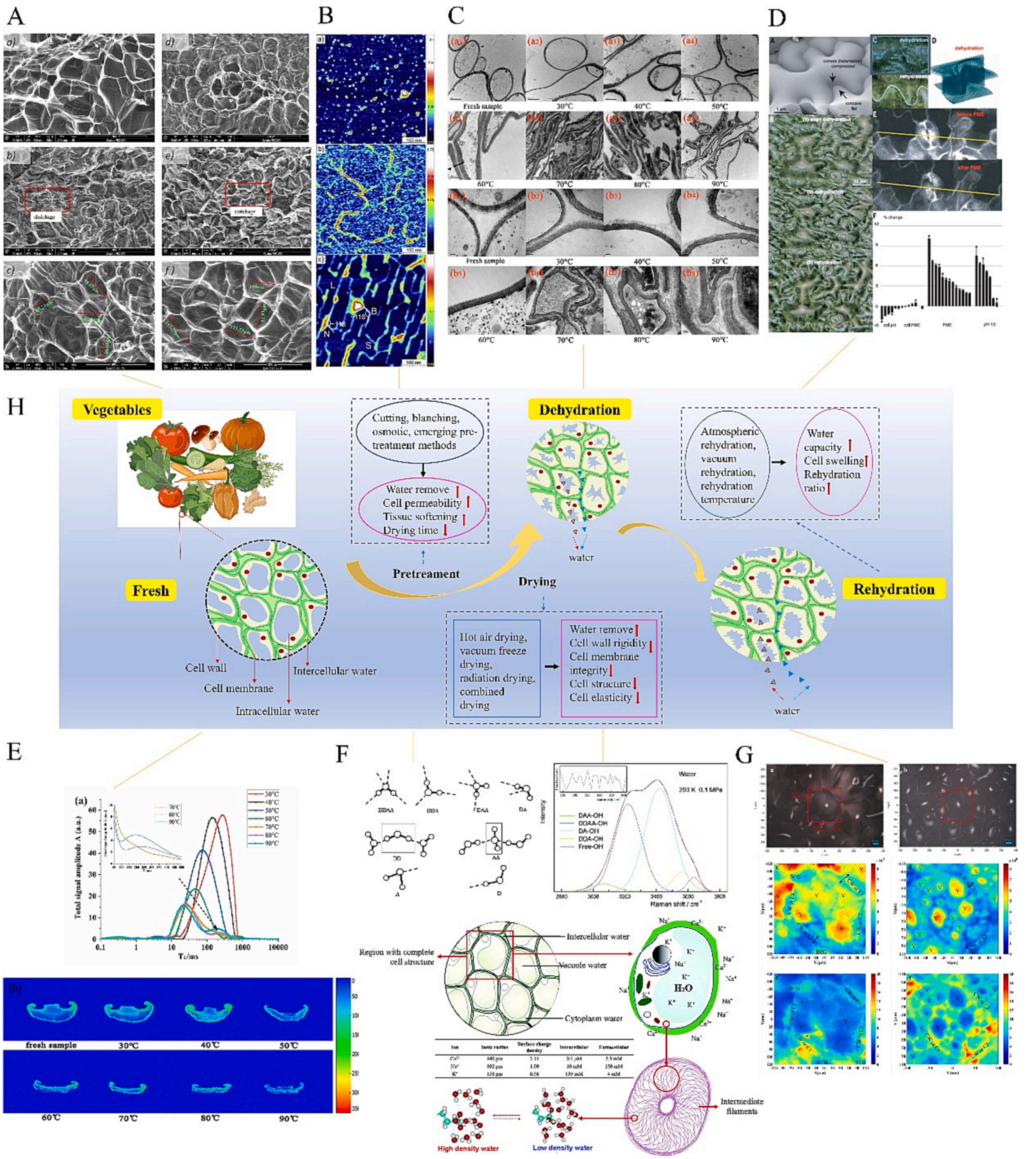

Fig. 3. Promising emerging analysis of microstructure and water migration in rehydration processes. A: Scanning electron microscope of pulsed electric fields-treated carrots. The figures were reproduced from Liu et al. (2020) with the permission from Elsevier. B: Atomic force microscopy of carrot pectin (a: WSP fraction; b: CSP fraction; c: DASP fraction) (500 × 500 nm scan). The figures were reproduced from Cybulska, Zdunek, and Kozioł (2015) with the permission from Elsevier. C: The transmission electron microscope microstructure observation of rehydrated shiitake mushrooms at different drying temperatures. The figures were reproduced from Qiu et al. (2021) with the permission from Elsevier. D: The changes in the cell walls of dehydrated and rehydrated plants were observed by cryo-SEM. The figures were reproduced from Haas et al. (2020) with the permission from AAAS. E: LF-NMR and MRI results of rehydrated samples at different drying temperature. The figures were reproduced from Qiu et al. (2021) with the permission from Elsevier. F: Types of hydrogen bonds formed with water molecules and water locates in the plant tissue. The figures were reproduced from Li et al. (2020) with the permission from Royal Soc Chemistry. G: CRM images of the water content distribution at the cellular level and the water state of different hydrogens. The figures were reproduced from Li, Zhu, and Sun (2022) with the permission from Elsevier. H: The flow chart for the whole process of vegetable dehydration to rehydration.

the rehydrated samples, also indicating that immobilized water became the dominant water state in the rehydrated samples. Moreover, new measurement and analysis techniques (such as LF-NMR and MRI) can better describe the characteristics of water migration during food rehydration (Zhao et al., 2019).

Researchers (Alolga et al., 2021; Feng et al., 2021; Monteiro, Link, Tribuzi, Carciofi, & Laurindo, 2018; Zhao et al., 2019) compared the effects of HAD with MVD, microwave multiple flash drying (MWMFD), VFD and infrared drying (FIRD) methods on pumpkin, garlic, banana, persimmon and mushroom, and found that the higher dehydration temperature during dehydration process resulted in poorer product quality and sensory quality. Therefore, HAD is not the best drying method for the improvement of rehydration process, and there are problems such as high energy consumption and environmental pollution. In recent years, scientific researchers have worked on better processing methods.

3.3.2. Effect of vacuum freeze drying on rehydration

VFD requires pre-freezing processing, pre-freezing temperature usually in the range of -45 ~ -30 °C, which has a great impact on the product quality (Mujumdar & Jangam, 2022). The ice crystals formed by slow freezing are larger. However, large ice crystals cause mechanical damage to the cell structure, the solute concentration effect that occurs during freezing may lead to protein denaturation, which reduce the elasticity and rehydration of dry products (Feng et al., 2020). In rapid freezing, relatively uniform and small ice crystals are formed, and the space left by ice sublimation is small, so the water vapor diffuse takes a long time, but the structural integrity is maintained, which may be conducive to the rehydration process. Therefore, the proper selection of pre-freezing process parameters should be considered in many aspects.

Some researchers studied the dehydration–rehydration of VFD carrots and found that VFD can lead to better connectivity of carrot pore structure, preserve the morphology of cell wall, and better rehydration capacity (Tan et al., 2021). Tan et al. (2021) and An et al. (2022) subjected tomatoes and edamame to different drying (including HAD, MRD, HMRD, PSMVD and VFD treatment, and the results showed that the VFD tomatoes (cultivar 18,131) and VFD edamame have better appearance, and the RR (VFD tomatoes: 3.83 ± 0.21; VFD edamame: 1.67 d.b.) of VFD samples is the largest compared with other dried samples (Table 2). This may be that the samples retained their original tissue structure after freeze-drying and that the samples maintained good water retention after rehydration. It is not certain that freeze-drying has good rehydration ability, and the RR vary depending on the nature of samples. After freezing, the properties of the samples themselves change, so they can't absorb enough water after rehydration processing, so the RR is low. In the future, we can analyze the water distribution and migration direction of samples properties and realize the appropriate drying method to achieve high RR products.

3.3.3. Effect of radiation drying on rehydration

Radiation drying methods include MD, FIRD and others, which utilize radiation energy to heat the food materials internally. So, the internal heating of the material allows the moisture to escape and the dried products can show a higher rehydration capacity. This is due to the shorter radiation drying time, resulting in smaller shrinkage. Zhao et al. (2019) found that infrared hot air drying (IRHAD) shiitake mushrooms had less surface hardening, higher rehydration, and greater brittleness than HAD. Moreover, the high moisture vapor pressure generated in the drying process results in a porous dried products with well-defined intercellular spaces, which absorbs large amounts of water during rehydration (İlter et al., 2018). Zhao et al. (2021) reported the rehydration of Lotus (Nelumbo nucifera Gaertn) seeds after drying by MVD at different US powers (6.08 w/cm^2, 8.39 w/cm^2, 10.84 W/cm^2) and found that the RR of the dried samples at power 10.84 w/cm^2 was about 0.85 d.b. (Table 2). The vibration effect positively affects drying, and a synergistic effect, where moisture transfer and the creation of more micro-porous channels are responsible for the increase in rehydration capacity.

3.3.4. Effect of combined drying on rehydration

Combined drying avoids the disadvantages of single drying method, and is a drying technology that combines two or more drying methods, including microwave-hot air combination (MDHAD), MWMFD, differential pressure flash drying-hot air and so on. Combined drying makes shrinkage, good integrity and color retention, strong rehydration capacity. Moreover, combined drying methods can shorten the drying time and save costs (Politowicz et al., 2018; Wei et al., 2019).

A study by Monteiro, Link, Tribuzi, Carciofi, & Laurindo (2018) reported that pumpkin slices were dried using MWMFD, microwave vacuum drying (MWVD), conductive multiple flash drying (KMFD), VFD and HAD. Rehydration of dried pumpkin slices revealed that MWMFD (29.34 g/g/h, 15.610 ± 1.008) and MWVD (38.38 g/g/h, 15.307 ± 0.580) had higher drying rate and RR than those of the KMFD (7.72 g/g/h, 5.781 ± 0.320), VFD (0.73 g/g/h, 10.450 ± 1.076) and HAD (1.71 g/g/h, 3.138 ± 0.456) samples (Table 2). The steam generated inside the product and the continuous heating of the vacuum pulse cycles cause the pumpkin to form a porous structure, thus facilitating the absorption of water during the rehydration process. Alolga et al. (2021) explored that the RR of the drying samples after V + US + OD + RHCD combined drying was the largest (RR: 11 ~ 12) compared with US + OD + RHCD drying (RR: 9 ~ 10) (Table 2). This may be the result of the synergistic effect of ultrasonic cavitation and osmotic pressure, which disrupts the cellular structure and facilitates the entry of water into the dried garlic slices through the formation of microchannels. Scanning electron microscope (SEM) can be used to observe the microstructure changes after rehydration (Hu et al., 2021). Feng et al. (2021) demonstrated that different drying methods had effects on garlic rehydration, with samples dried by IRHAD exhibit the higher RR (RR: 2.00) than HAD (RR: 1.82) (Table 2). Moreover, the microstructure images of rehydrated garlic samples can visually demonstrate the changes in rehydration capacity (Fig. 2D). IRHAD homogeneous heating causes little damage to cell structure, which reduces the loss of biological activity and improves the rehydration capacity.

Sample characteristics should be considered when pre-treatment samples. For samples with high color requirements, osmotic pretreatment with ethanol should be avoided, as this may lead to color degradation. This is because ethanol has a decolorizing effect (Islam, Arioli, & Cahill, 2021). In the selection of osmotic solution, the quality of the sample after rehydration and consumer taste requirements should also be considered. Different drying methods also have important effects on the RR of the samples, which can be seen from the literature summary of drying methods and rehydration ratio of dried samples (Table 2). In recent years, the combined drying methods have been applied more and more, which has the best microstructure performance, and the sample has a high moisturizing ability after rehydration (Hu, Bi, Jin, Qiu, & Sman, 2021). Moreover, combined drying can improve the RR of vegetables. However, the connection between several drying methods deserves attention. The effect of combined drying method on rehydration process is less studied, and the rehydration kinetics needs further exploration. Dehydrated products with low cost, low consumption, environmental friendliness and high quality are favored. With the continuous research and exploration of rehydration processing, different emerging technology and equipment will be constantly updated and expanded for the benefit of mankind.

3.4. Rehydration conditions

The good tissue state and taste of the rehydrated vegetables are inseparable from the rehydration method and rehydration conditions. In recent years, there has been limited research on rehydration methods and conditions. The commonly explored methods include atmospheric rehydration and vacuum rehydration. And the rehydration conditions are mainly controlling the rehydration temperature (Zhou et al., 2021).

Rehydration methods: The rehydration methods include atmospheric rehydration and vacuum rehydration. Vacuum RR is higher mainly for two reasons, (1) vacuum pressure promotes the softness of fibers and other tissues, enhances the formation of larger cavities, facilitates cell expansion, and increases water capacity. (2) pressure difference in a vacuum environment allows dehydrated vegetables to absorb water more rapidly. Zhou et al. (2021) demonstrated that the RR after vacuum rehydration (HAD vacuum rehydration: ~3, VFD vacuum rehydration) was greater than the RR at atmospheric pressure (HAD normal rehydration: ~2, VFD normal rehydration: ~2) (Table 2). García-Segovia and Martínez-Monzó (2011) found that the rate of vacuum rehydration was faster than normal rehydration, possibly due to the effect of pressure on cell expansion. The vacuum effect helps to the softening fiber tissue and increase cavity and water volume. The rapid rehydration and filling of cavities (intercellular spaces) near the surface is facilitated by the vacuum process, which helps to remove the air bubbles trapped in the cavities. There are few studies on vacuum rehydration, and the correlation between vacuum pressure and the properties of the rehydrated product as well as the study of vacuum rehydration mechanism deserves more attention.

Rehydration temperature: Appropriately increasing the rehydration water temperature of dehydrated vegetables can promote the water diffusion or capillary action, shorten the rehydration time and improve the rehydration capacity (Pramiu, Rizzi, Antunes, Denes, & Coelho, 2018). According to Monteiro, Link, Tribuzi, Carciofi, & Laurindo (2018), RR (3.138 ~ 3.968) of HAD pumpkins increased with higher rehydration temperature (25 ~ 80 °C). This indicates that the rehydration temperature has an impact on the RR. The RR of the dried KMFD pumpkin samples at 80 °C (6.117 ± 0.125) was significantly higher than that at 25 °C (5.781 ± 0.320) after rehydration (Table 2). However, rehydration process at higher temperature leads to structural destruction of the dehydrated product, which hinders water absorption. This structural damage reduces the number and size of capillary pathways or pores, and thus the role of the capillaries, which affects the RR. Meanwhile, the increase of rehydration temperature significantly reduces the mechanical resistance of sample, aggravates the structural damage during thermal dehydration and leads to textural deterioration. RR is also related to drying method and drying temperature. Rehydration of low porosity (HAD) products is mainly due to diffusion, while the products with high porosity (VFD) is mainly due to capillarity (García-Segovia & Martínez-Monzó, 2011).

Benseddik et al. (2019) evaluated the Weibull model of rehydration for pumpkin slices prepared with different drying methods. For all the different drying samples, the β value of HAD, vacuum multiple flash drying (VMFD) and swell-drying decreased from 67.378 to 3.872 min when the rehydration temperature increased from 30 °C to 60 °C, indicating that rehydration reaches equilibrium faster as the rehydration temperature is increased. However, it was found that the β value of VFD pumpkin slices increased after the rehydration temperature was increased from 45 °C, which might be due to the rehydration temperature and drying methods affecting the rehydration process. The correlation between structure and mass transfer phenomenon during rehydration process remains to be further investigated. Currently, studies on rehydration temperature have focused on the completion of the rehydration process at constant temperature. However, for some dehydrated vegetables, it is possible that rehydration at different temperature conditions may shorten the rehydration time and improve the quality of the rehydrated vegetables. There are few studies on variable temperature, and future researches on rehydration kinetics of variable temperature and rehydration processes are necessary to facilitate production innovation.

Reversible or irreversible cell deformation and dislocation are observed during pre-treatment, drying and rehydration, which may lead to the destruction of cell integrity and strong contraction of capillaries, thus affecting the quality of vegetables (Górnicki, Choińska, & Kaleta, 2020). The study conducted by Haas, Wightman, Meyerowitz, & Peaucelle (2020), they used cryo-SEM to observe the changes in cell walls of dehydrated and rehydrated plants (Fig. 3D), the results showed that the changes in the cells following drying and rehydration were associated with variations in cell wall composition and swelling pressure. Cell wall and cell membrane are important components supporting the structure of vegetable, and we speculate that this is also an important factor affecting the dehydration–rehydration process. Clarification the relationship between dehydration–rehydration process and cell structure contribute to vegetables processing. More importantly, control the process strictly, we can significantly improve the vegetables quality, leading to increased efficiency and economic benefit. Thus, the changes of the cell structure during dehydration-rehydration process need a lot of researches.

4. Challenges and future prospects

Previous studies have found that pre-treatments, drying, and rehydration methods have a significant impact on the quality of the rehydrated product. We also found some changes in microstructure and moisture detection, but rehydration studies still face some challenges.

4.1. Exploring dehydration-rehydration mechanism from cell structure

Interestingly, for some dehydrated vegetables (e.g., dried cucumbers), a certain degree of dehydration results in better taste, and the analysis of the correlation between cucumber water loss and taste after cooking (rehydration) is worth investigating. It is necessary to clarify the mechanism of dehydration and rehydration of vegetables. Improving the quality of dehydrated vegetables can be considered in terms of cell structure (e.g., cell membrane and cell wall). Furthermore, we can get some thoughts from the flow chart of the whole process of vegetable dehydration to rehydration (Fig. 3H). In the study of Cybulska, Zdunek, and Kozioł (2015), the water-soluble (WSP), chelator-soluble (CSP) and dilute alkali-soluble pectin (DASP) components of carrot cell walls were characterized by AFM. It was found that WSP contains a high proportion of small pectin polymers, while DASP molecules on mica showed a regular network in the early mature tissues, and CSP fraction contains a mixture of both chains and also contained short polymer structure (Fig. 3B). In further research, we can also use AFM to explore the changes in the internal composition of ell structure under different processing conditions, and thus better control the parameters of the processing process and obtain high-quality vegetable products. The influence of cell components and morphological (e.g., pectin and fiber) on the quality of dehydrated vegetables during the rehydration process is still unclear. In-depth analysis of the relationship between rehydration and restorability including the structural and compositional of cell walls and cell membranes.

4.2. New technology for rehydration

In addition, the main rehydration methods studied so far are atmospheric pressure rehydration and vacuum rehydration (Zhou et al., 2021), with fewer combined methods. Future continued researches can explore emerging rehydration process in combination with pre-treatment technologies, such as US, microwave, and some non-thermal methods (such as, PEF, CP and low-frequency ultrasound) (Bassey, Cheng, & Sun, 2021). For some color sensitivity vegetables in pre-treatment, drying way process are carried out non-thermal treatment, so in the rehydration process also ensure the rehydration speed, shorten the rehydration process. These techniques can be explored as rehydration methods in future researches. Moreover, mathematical modeling methods can be used to reduce the number of experiments, to provide guiding information for developing these new rehydration techniques.

Raman spectroscopy has been used to study the hydrogen bonding state of water molecules. In the current study, a novel technique for

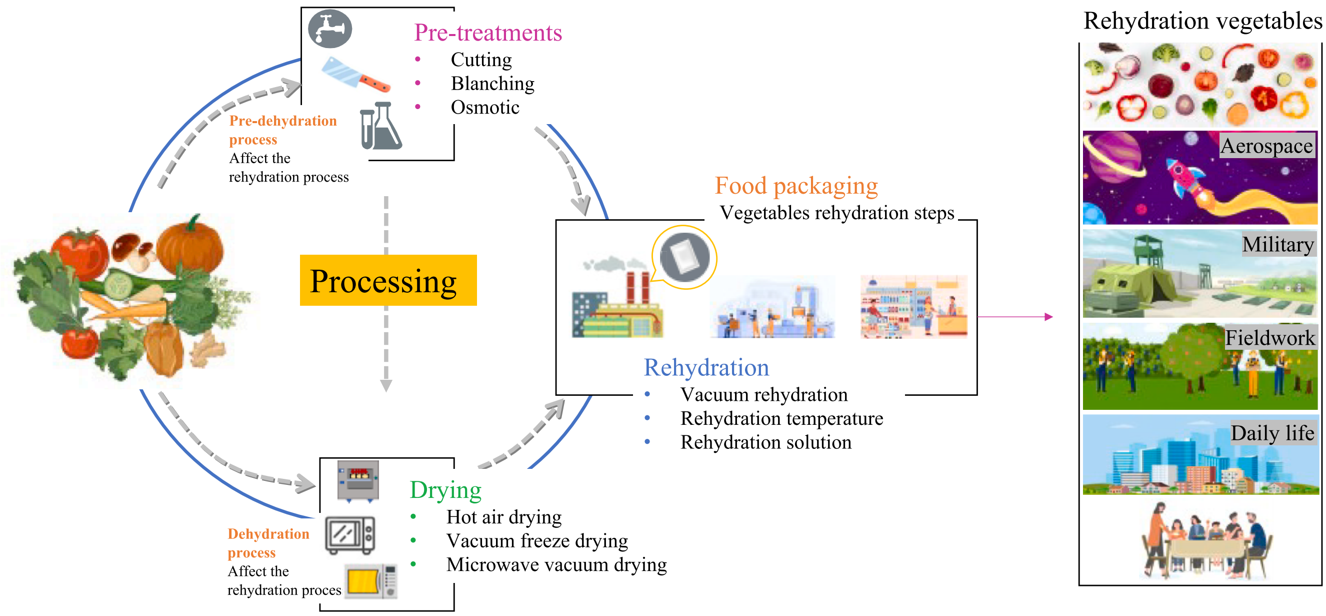

Fig. 4. Industrialized production to achieve the integration of rehydrated convenience foods from processing to the table.

confocal Raman microscopy (CRM) imaging was developed to determine the distribution of water content at the cellular level and the water state of various hydrogens (Li, Zhu, & Sun, 2021). In the study of Li, Zhu, and Sun (2020), Raman data obtained from apple cells were calculated as the area of OH stretching vibration and the ratio of DA-OH to DDAA-OH stretching vibration area or the number of hydrogen bonds per water molecule using the fixed-position (Fig. 3F). According to Li, Zhu, and Sun (2022), the distribution of water and hydrogen bonding states in apple and potato cells were determined using CRM, and the differences in water distribution in these cells were compared. Moreover, the total water content, free water content and hydrogen bonding state of free water were determined quantitatively (Fig. 3G). The size of the water presence region has a significant effect on the hydrogen bonding state of water. CRM imaging can be used to analyze the water distribution and hydrogen bond status in future rehydrated products to find a suitable way for vegetable rehydration.

4.3. Packaging identification of complex rehydration products

Due to the complexity of vegetables, applying the same rehydration method to all vegetables to achieve satisfactory results is a challenge. The current study focuses on rehydration of singular vegetable (Alolga et al., 2021; Qiu et al., 2021). Therefore, it is necessary to group vegetables according to their shape and type to establish a protocol for the most suitable rehydration method for each group, which may provide a satisfactory method for improving the quality of the rehydrated products.

The recoverability of vegetables is closely related to pre-treatment, drying, and rehydration methods due to the processing characteristics of vegetables (Obajemihi et al., 2023). For example, during improper drying process, the vegetable cells may be irreversibly damaged and collapsed, thus preventing sufficient absorption of water due to cell destruction during rehydration and affecting the quality of the rehydrated product. Future researches can focus on establishing standards to form a kind of standardization of pre-treatment, drying and rehydration methods. This will not only ensure the value of vegetables but also bring convenience to people. Moreover, standardization can be applied to factories for production. By precisely adjusting process parameters, industrial production can combine pre-treatment and drying methods with product packaging to ensure a seamless transition from process to table. In addition, the rehydration method is marked on the packaging and provided for consumption on specific occasions, such as aerospace, military, field operations and daily life, etc. (Fig. 4). Aspects of food is promising, more and more simple rehydration of vegetable foods is the future development needs.

5. Conclusions

This review provides detailed review of the rehydration process of vegetables, which was described by three model: Fick diffusion law, Peleg model and Fick Weibull mode. It is worth noting that the rehydration process of vegetables is temperature dependent. Different rehydration models were compared to explore a model suitable for predicting the rehydration characteristics of vegetables. It is expected to provide practical guidance on the rehydration process of vegetables, which will be beneficial to the development of instant food with rehydrated vegetables.

It is believed that perforation is the best cutting method for pre-treatment, and that proper blanching temperature and time as well as compound permeation solution are beneficial to the quality of rehydrated vegetables. Combined drying is the preferred drying method, which has the good microstructure performance, and high rehydration capacity for vegetables. Suitable rehydration methods help to ensure the quality of rehydrated vegetable products, as well as saving energy and significantly improving the reducibility of the vegetables. Variable temperature in the rehydration process can be considered in the future, which may shorten the rehydration time and improve the quality of the vegetables.

The structure and composition of cell walls and cell membranes are key points for future exploration of dehydration-rehydration mechanisms. The emerging detection methods of rehydrated vegetables are summarized, among which CRM is a promising technique to study water changes, and the hydrogen bond and water state of vegetable cells after rehydration deserve further study. Furthermore, personalized rehydration packaging to meet the needs of is future development direction. These efforts can lead to a better understanding of the rehydration process.

CRediT authorship contribution statement

Bixiang Wang: Investigation, Formal analysis, Writing – original draft. **Yuanlong Jia:** Formal analysis, Writing – review & editing. **Yue**

Li: Investigation, Writing – review & editing. **Zhitong Wang:** Investigation, Writing – review & editing. **Liankui Wen:** Conceptualization, Project administration, Writing – review & editing. **Yang He:** Conceptualization, Supervision, Formal analysis, Writing – review & editing. **Xiuying Xu:** Conceptualization, Formal analysis, Writing – review & editing.

Declaration of Competing Interest

The authors declare that they have no known competing financial interests or personal relationships that could have appeared to influence the work reported in this paper.

Data availability

No data was used for the research described in the article.

Acknowledgment

This work was supported by the Jilin Scientific and Technological Development Program [grant number 20230202047NC]. And we also thank the Jilin Agricultural University Agricultural Products Processing and Storage Laboratory for support.

Appendix A. Supplementary data

Supplementary data to this article can be found online at https://doi.org/10.1016/j.fochx.2023.100935.

References

Alolga, R. N., Osae, R., Essilfie, G., Saalia, F. K., Akaba, S., & Chikari, F. (2021). Sonication, osmosonication and vacuum-assisted osmosonication pretreatment of Ghanaian garlic slices: Effect on physicochemical properties and quality characteristics. *Food Chemistry, 343*, Article 128535. https://doi.org/10.1016/j.foodchem.2020.128535

Andreou, V., Dimopoulos, G., Dermesonlouoglou, E., & Taoukis, P. (2020). Application of pulsed electric fields to improve product yield and waste valorization in industrial tomato processing. *Journal of Food Engineering, 270*, Article 109778. https://doi.org/10.1016/j.jfoodeng.2019.109778

An, N.-N., Sun, W.-H., Li, B.-Z., Wang, Y., Shang, N., Lv, W.-Q., … Wang, L.-J. (2022). Effect of different drying techniques on drying kinetics, nutritional components, antioxidant capacity, physical properties and microstructure of edamame. *Food Chemistry, 373*, Article 131412. https://doi.org/10.1016/j.foodchem.2021.131412

Aravindakshan, S., Kyomugasho, C., Buvé, C., van Loey, A., & Hendrickx, M. (2021). The impact of drying and rehydration on the structural properties and quality attributes of pre-cooked dried beans. *Foods*, *10*(7), 1665. https://doi.org/ 10.3390/foods10071665.

Ansari, S., Maftoonazad, N., Farahnaki, A., Hosseini, E., & Asadi, G. (2015). Modeling Rehydration Behavior of Dried Figs. *Journal of Agricultural Science and Technology, 17* (1), 133–144. https://doi.org/10.1007/BF02723037

Bassey, E. Z., Cheng, J. H., & Sun, D. W. (2021). Novel nonthermal and thermal pretreatments for enhancing drying performance and improving quality of fruits and vegetables. *Trends in Food Science & Technology, 112*, 137–148. https://doi.org/10.1016/j.tifs.2021.03.045

Benseddik, A., Azzi, A., Zidoune, M. N., Khanniche, R., & Besombes, C. (2019). Empirical and diffusion models of rehydration process of differently dried pumpkin slices. *Journal of the Saudi Society of Agricultural Sciences, 18*(4), 401–410. https://doi.org/10.1016/j.jssas.2018.01.003

Biswas, R., Hossain, M. A., & Zzaman, W. (2022). Thin layer modeling of drying kinetics, rehydration kinetics and color changes of osmotic pre-treated pineapple (Ananas comosus) slices during drying: Development of a mechanistic model for mass transfer. *Innovative Food Science & Emerging Technologies, 80*, Article 103094. https://doi.org/10.1016/j.ifset.2022.103094

Bozkir, H., & Ergün, A. R. (2020). Effect of sonication and osmotic dehydration applications on the hot air drying kinetics and quality of persimmon. *LWT- Food Science and Technology, 131*, Article 109704. https://doi.org/10.1016/j.lwt.2020.109704

Bozkir, H., Ergün, A. R., Serdar, E., Metin, G., & Baysal, T. (2019). Influence of ultrasound and osmotic dehydration pretreatments on drying and quality properties of persimmon fruit. *Ultrasonics Sonochemistry, 54*, 135–141. https://doi.org/10.1016/j.ultsonch.2019.02.006

Bruce, D. M. (1985). Exposed-layer barley drying, three models fitted to new data up to 150 °C. *Journal of Agricultural Engineering Research. 32*(4), 337–347. https://doi.org/10.1016/0021-8634(85)90098-8.

Brunauer, S., Emmett, P. H., & Teller, E. (1938). Adsorption of Gases in Multimolecular Layers. *Journal of the American Chemical Society, 60*(2), 309–319. https://doi.org/10.1021/ja01269a023

Chen, D., Xing, B., Yi, H., Li, Y., Zheng, B., Wang, Y., & Shao, Q. (2020). Effects of different drying methods on appearance, microstructure, bioactive compounds and aroma compounds of saffron (Crocus sativus L.). *LWT- Food Science and Technology, 120*, Article 108913. https://doi.org/10.1016/j.lwt.2019.108913

Crank, J. (1975). *The Mathematics of Diffusion* (2nd ed.). London, UK: Oxford University Press.

Cybulska, J., Zdunek, A., & Kozioł, A. (2015). The self-assembled network and physiological degradation of pectins in carrot cell walls. *Food Hydrocolloids, 43*, 41–50. https://doi.org/10.1016/j.foodhyd.2014.04.032

Demiray, E., & Tulek, Y. (2017). Effect of temperature on water diffusion during rehydration of sun-dried red pepper (Capsicum annuum L.). *Heat and Mass Transfer, 53*(5), 1829–1834. https://doi.org/10.1007/s00231-016-1940-0

Demirhan, E., & Özbek, B. (2010). Rehydration kinetics of microwave-dried basil. *Journal of Food Processing and Preservation*, *34*(4), 664–680. https://doi.org/10.1111/j.1745-4549.2009.00384.x.

Deng, L. Z., Mujumdar, A. S., Yang, X. H., Wang, J., Zhang, Q., Zheng, Z. A., … Xiao, H.-W. (2018). High humidity hot air impingement blanching (HHAIB) enhances drying rate and softens texture of apricot via cell wall pectin polysaccharides degradation and ultrastructure modification. *Food Chemistry, 261*, 292–300. https://doi.org/10.1016/j.foodchem.2018.04.062

Deng, L. Z., Mujumdar, A. S., Zhang, Q., Yang, X. H., Wang, J., Zheng, Z. A., Gao, Z. J., & Xiao, H. W. (2019). Chemical and physical pretreatments of fruits and vegetables: Effects on drying characteristics and quality attributes–a comprehensive review. *Critical Reviews in Food Science and Nutrition, 59*(9), 1408–1432. https://doi.org/10.1080/10408398.2017.1409192

Deng, L. Z., Pan, Z., Mujumdar, A. S., Zhao, J. H., Zheng, Z. A., Gao, Z. J., & Xiao, H. W. (2019). High-humidity hot air impingement blanching (HHAIB) enhances drying quality of apricots by inactivating the enzymes, reducing drying time and altering cellular structure. *Food Control, 96*, 104–111. https://doi.org/10.1016/j.foodcont.2018.09.008

Duckworth, R. B. (1975). *Water relations of Foods*. Academic Press.

Fan, K., & Zhang, M. (2019). Recent developments in the food quality detected by non-invasive nuclear magnetic resonance technology. *Critical Revie-ws in Food Science and Nutrition, 59*(14), 2202–2213. https://doi.org/10.1080/10408398.2018.1441124

FAO, FAOSTAT. Crop statistics are recorded for 173 products, covering the following categories: Crops Primary, Fibre Crops Primary, Cereals, Coarse Grain, Citrus Fruit, Fruit, Jute Jute-like Fibres, Oilcakes Equivalent, Oil crops Primary, Pulses, Roots and Tubers, Treenuts and Vegetables and Melons. Data are expressed in terms of area harvested, production quantity and yield. 2022a, 5, 17. https://www.fao.org/faostat/zh/#data/QCL/visualize.

FAO, FAOSTAT. The food and agricultural trade dataset is collected, processed and disseminated by FAO according to the standard International Merchandise Trade Statistics (IMTS) Methodology. 2022b, 5, 17. https://www.fao.org/faostat/zh/#data/TCL.

Feng, Y., Ping Tan, C., Zhou, C., Yagoub, A. E. A., Xu, B., Sun, Y., … Yu, X. (2020). Effect of freeze-thaw cycles pretreatment on the vacuum freeze-drying process and physicochemical properties of the dried garlic slices. *Food Chemistry, 324*, Article 126883. https://doi.org/10.1016/j.foodchem.2020.126883

Feng, Y., Xu, B. G., Yagoub, A. E., Ma, H., Sun, Y., Xu, X., Yu, X. J., & Zhou, C. S. (2021). Role of drying techniques on physical, rehydration, flavor, bioactive compounds and antioxidant characteristics of garlic. *Food Chemistry, 343*, Article 128404. https://doi.org/10.1016/j.foodchem.2020.128404

Feng, Y., Zhou, C., ElGasim A. Yagoub, A., Sun, Y., Owusu-Ansah, P., Yu, X., . . . Ren, Z. (2019). Improvement of the catalytic infrared drying process and quality characteristics of the dried garlic slices by ultrasound-assisted alcohol pretreatment. *LWT*, *116*, 108577. https://doi.org/10.1016/j.lwt.2019.108577.

García-Segovia, P., Andrés-Bello, A., & Martínez-Monzó, J. (2011). Rehydration of air-dried Shiitake mushroom (Lentinus edodes) caps: Comparison of conventional and vacuum water immersion processes. *LWT - Food Science and Technology, 44*(2), 480–488. https://doi.org/10.1016/j.lwt.2010.08.010

Górnicki, K., Choińska, A., & Kaleta, A. (2020). Effect of variety on rehydration characteristics of dried apples. *Processes, 8*, 1–21. https://doi.org/10.3390/pr8111454

Haas, K. T., Wightman, R., Meyerowitz, E., & Peaucelle, A. (2020). Pectin homogalacturonan nanofilament expansion drives morphogenesis in plant epidermal cells. *Science, 367*, 1003–1007. https://doi.org/10.1126/science.aaz5103

Harkins, W. D., & Jura, G. (1944). Surfaces of solids. XIII. A vapor adsorption method for the determination of the area of a solid without the assumption of a molecular area, and the areas occupied by nitrogen and other molecules on the surface of a solid. *Journal of the American Chemical Society*, *66*(8), 1366–1373. https://doi.org/10.1021/ja01236a048.

Henderson, S. M. (1974). Progress in developing the thin layer drying equation. *Transactions of the American Society of Agricultural Engineers*, *17*(6) 1167–1168. https://doi.org/ 10.13031/2013.37052.

Henderson, S. M., & Pabis, S. (1961). Grain drying theory I: Temperature effect on drying coefficient. *Journal of Agricultural Engineering Research, 6*, 169–174.

Hu, L., Bi, J., Jin, X., Qiu, Y., & Sman, R. (2021). Study on the rehydration quality improvement of shiitake mushroom by combined drying methods. *Foods, 10*, 769. https://doi.org/10.3390/foods10040769

Hukill, W. V. (1954). Grain drying. in: J.A., Anderson, A.W. Alcock (Eds.), Storage of cereal grain and their products. Amer. Ass. Cereal Chem, St. Paul, Minn.

İlter, I., Akyıl, S., Devseren, E., Okut, D., Koç, M., & Kaymak Ertekin, F. (2018). Microwave and hot air drying of garlic puree: Drying kinetics and quality characteristics. *Heat and Mass Transfer, 54*(7), 2101–2112. https://doi.org/10.1007/s00231-018-2294-6

Islam, M. T., Arioli, T., & Cahill, D. M. (2021). Seaweed Extract-Stimulated Priming in Arabidopsis thaliana and Solanum lycopersicum. *Plants (Basel), 10*(11), 2476. https://doi.org/10.3390/plants10112476

Kayacan, S., Karasu, S., Akman, P. K., Goktas, H., Doymaz, I., & Sagdic, O. (2020). Effect of different drying methods on total bioactive compounds, phenolic profile, in vitro bioaccessibility of phenolic and HMF formation of persimmon. *LWT, 118*, Article 108830. https://doi.org/10.1016/j.lwt.2019.108830

Khan, M. I. H., Farrell, T., Nagy, S. A., & Karim, M. A. (2018). Fundamental understanding of cellular water transport process in bio-food material during Drying. *Science Reports, 8*(1), 15191. https://doi.org/10.1038/s41598-018-33159-7

Khan, M. I. H., Nagy, S. A., & Karim, M. A. (2018). Transport of cellular water during drying: An understanding of cell rupturing mechanism in apple tissue. *Food Research International, 105*, 772–781. https://doi.org/10.1016/j.foodres.2017.12.010

Kumar, Y., Singh, L., Sharanagat, V. S., Mani, S., Kumar, S., & Kumar, A. (2021). Quality attributes of convective hot air dried spine gourd (Momordica dioica Roxb. Ex Willd) slices. *Food Chemistry*, *347*, 129041. https://doi.org/10.1016/j.foodchem.2021.129041.

Labuza, T. P. (2007). The properties of water in relationship to water binding in foods: A review. *Journal of Food Processing and Preservation, 1*(2), 167–190. https://doi.org/10.1111/j.1745-4549.1977.tb00321.x

Lech, K., Adam, F., Michalska, A., Wojdyło, A., & Nowicka, P. (2018). The effect of selected fruit juice concentrates used as osmotic agents on the drying kinetics and chemical properties of vacuum-microwave drying of pumpkin. *Journal of Food Quality, 1–11*. https://doi.org/10.1155/2018/7293932

Li, D. T., Deng, L. Z., Dai, T. T., Chen, M. S., Liang, R. H., Liu, W., Liu, C. M., Chen, J., & Sun, J. (2022). Ripening induced degradation of pectin and cellulose affects the far infrared drying kinetics of mangoes. *Carbohydrate Polymers, 291*, Article 119582. https://doi.org/10.1016/j.carbpol.2022.119582

Li, D., Zhu, Z., & Sun, D.-W. (2020). Visualization of the in situ distribution of contents and hydrogen bonding states of cellular level water in apple tissues by confocal Raman microscopy. *The Analyst, 145*(3), 897–907. https://doi.org/10.1039/C9AN01743G

Li, D., Zhu, Z., & Sun, D. W. (2021). Quantification of hydrogen bonding strength of water in saccharide aqueous solutions by confocal Raman microscopy. *Journal of Molecular Liquids, 342*, Article 117498. https://doi.org/10.1016/j.molliq.2021.117498

Li, D., Zhu, Z., & Sun, D. W. (2022). Visualization and quantification of content and hydrogen bonding state of water in apple and potato cells by confocal Raman microscopy: A comparison study. *Food Chemistry, 385*, Article 132679. https://doi.org/10.1016/j.foodchem.2022.132679

Li, M., Wang, B., Lv, W., & Zhao, D. (2022) Effect of ultrasound pretreatment on the drying kinetics and characteristics of pregelatinized kidney beans based on microwave-assisted drying. *Food Chemistry*, 397, 133806. https://doi: 10.1016/j.foodchem.2022.133806.

Li, S., Chen, S., Liang, Q., Ma, Z., Han, F., Xu, Y., Jin, Y., & Wu, W. (2019). Low temperature plasma pretreatment enhances hot-air drying kinetics of corn kernels. *Journal of Food Process Engineering, 42*(6), e13195.

Liu, C., Pirozzi, A., Ferrari, G., Vorobiev, E., & Grimi, N. (2020). Impact of pulsed electric fields on vacuum drying kinetics and physicochemical properties of carrot. *Food Research International, 137*, Article 109658. https://doi.org/10.1016/j.foodres.2020.109658

Liu, J., Bi, J., McClements, D. J., Liu, X., Yi, J., Lyu, J., … Liu, D. (2020). Impacts of thermal and non-thermal processing on structure and functionality of pectin in fruit- and vegetable- based products: A review. *Carbohydrate Polymers, 250*, Article 116890. https://doi.org/10.1016/j.carbpol.2020.116890

Llavata, B., García-Pérez, J. V., Simal, S., & Cárcel, J. A. (2020). Innovative pre-treatments to enhance food drying: A current review. *Current Opinion in Food Science, 35*, 20–26. https://doi.org/10.1016/j.cofs.2019.12.001

Lopez-Quiroga, E., Prosapio, V., Fryer, P. J., Norton, I. T., & Bakalis, S. (2019). A model-based study of rehydration kinetics in freeze-dried tomatoes. *Energy Procedia, 161*, 75–82. https://doi.org/10.1016/j.egypro.2019.02.060

Machado, M., Oliveira, F. A. R., Gekas, V., & Singh, R. P. (1998). Kinetics of moisture uptake and soluble-solids loss by puffed breakfast cereals immersed in water. *International Journal of Food Science & Technology, 33*(3), 225–237. https://doi.org/10.1046/j.1365-2621.1998.00197.x

Managa, M. G., Sultanbawa, Y., & Sivakumar, D. (2020). Effects of different drying methods on untargeted phenolic metabolites, and antioxidant activity in Chinese cabbage (Brassica rapa L. subsp. chinensis) and Nightshade (Solanum retroflexum Dun.). *Molecules*, *25*(6). https://doi.org/10.3390/molecules25061326.

Maneesh Kumar, M., Prasad, K., Sarat Chandra, T., & Debnath, S. (2018). Evaluation of physical properties and hydration kinetics of red lentil (Lens culinaris) at different processed levels and soaking temperatures. *Journal of the Saudi Society of Agricultural Sciences, 17*(3), 330–338. https://doi.org/10.1016/j.jssas.2016.07.004

Markowski, M., Stankiewicz, I., Zapotoczny, P., & Borowska, J. (2006). Effect of variety on drying characteristics and selected quality attributes of dried carrots. *Drying Technology, 24*(8), 1011–1018. https://doi.org/10.1080/07373930600776191

Miano, A. C., Rojas, M. L., & Augusto, P. E. D. (2021). Combining ultrasound, vacuum and/or ethanol as pretreatments to the convective drying of celery slices. *Ultrasonics Sonochemistry, 79*, Article 105779. https://doi.org/10.1016/j.ultsonch.2021.105779

Monteiro, R. L., Link, J. V., Tribuzi, G., Carciofi, B. A. M., & Laurindo, J. B. (2018). Microwave vacuum drying and multi-flash drying of pumpkin s-lices. *Journal of Food Engineering, 232*, 1–10. https://doi.org/10.1016/j.jfoodeng.2018.03.015

Mujumdar, A. S., & Erdesz, K. (2007). Applications of vibration techniques for drying and agglomeration in food processing. *Drying Technology-An International Journal, 6*, 255–274.

Nowacka, M., Laghi, L., Rybak, K., Dalla Rosa, M., Witrowa-Rajchert, D., & Tylewicz, U. (2019). Water state and sugars in cranberry fruits subjected to combined treatments: Cutting, blanching and sonication. *Food Chemistry, 299*, Article 125122. https://doi.org/10.1016/j.foodchem.2019.125122

Obajemihi, O. I., Esua, O. J., Cheng, J. H., & Sun, D. W. (2023). Effects of pretreatments using plasma functionalized water, osmodehydration and their combination on hot air drying efficiency and quality of tomato (Solanum lycopersicum L.) slices. *Food Chemistry*, *406*, 134995. https://doi.org/ 10.1016/j.foodchem.2022.134995.

Osae, R., Alolga, R. N., Essilfie, G., Osei-Adjei, G., Baduweh, C. A., Yarley, O. P. N., & Zhou, C. (2020a). Variation in bioactive phytochemicals and sensory attributes of osmosonic convective dried ginger from four African countries. *Journal of the Science of Food and Agriculture, 100*(7), 3164–3172. https://doi.org/10.1002/jsfa.10351

Osae, R., Essilfie, G., Alolga, R. N., Akaba, S., Song, X., Owusu-Ansah, P., & Zhou, C. (2020b). Application of non-thermal pretreatment techniques on agricultural products prior to drying: A review. *Journal of the Science of Food and Agriculture, 100*(6), 2585–2599. https://doi.org/10.1002/jsfa.10284

Peleg, M. (1988). An empirical model for the description of moisture sorption curves. *Journal of Food Science, 53*(4), 1216–1217. https://doi.org/10.1111/j.1365-2621.1988.tb13565.x

Page, G. E. Factors influencing the maximum rates of air drying shelled corn in thin layers. 1949.

Politowicz, J., Lech, K., Sánchez-Rodríguez, L., Figiel, A., Szumny, A., Grubor, M., & Carbonell-Barrachina, Á. A. (2018). Volatile composition and sensory profile of oyster mushroom as affected by drying method. *Drying Technology, 36*(6), 685–696. https://doi.org/10.1080/07373937.2016.1274903

Pramiu, P. V., Rizzi, R. L., Antunes, F. C. A., Denes, F. M., & Coelho, S. R. M. (2018). Solutions and parameterizations of common bean (Phaseolus vulgaris) rehydration models at different temperatures and pressures. *Journal of Food Processing and Preservation, 42*(2), e13376.

Qiu, Y., Bi, J., Jin, X., Hu, L., Lyu, J., & Wu, X. (2021). An understanding of the changes in water holding capacity of rehydrated shiitake mushroom (Lentinula edodes) from cell wall, cell membrane and protein. *Food Chemistry, 351*, Article 129230. https://doi.org/10.1016/j.foodchem.2021.129230

Rahaman, A., Zeng, X.-A., Kumari, A., Rafiq, M., Siddeeg, A., Manzoor, M. F., … Ahmed, Z. (2019). Influence of ultrasound-assisted osmotic dehydration on texture, bioactive compounds and metabolites analysis of plum. *Ultrasonics Sonochemistry, 58*, Article 104643. https://doi.org/10.1016/j.ultsonch.2019.104643

Rahman, M. S., Perera, C. O., & Theband, C. (1998). Desorption isotherm and heat pump drying kinetics of peas. *Food Research International, 30*(7), 485–491. https://doi.org/10.1016/S0963-9969(98)00009-X

Ren, M., Ren, Z., Chen, L., Zhou, C., Okonkwo, C. E., & Mujumdar, A. S. (2022). Comparison of ultrasound and ethanol pretreatments before catalytic infrared drying on physicochemical properties, drying, and contamination of Chinese ginger (Zingiber officinale Roscoe). *Food Chemistry, 386*, Article 132759. https://doi.org/10.1016/j.foodchem.2022.132759

Rojas, M. L., & Augusto, P. E. D. (2018a). Ethanol and ultrasound pre-treatments to improve infrared drying of potato slices. *Innovative Food Science & Emerging Technologies, 49*, 65–75. https://doi.org/10.1016/j.ifset.2018.08.005

Rojas, M. L., & Augusto, P. E. D. (2018b). Ethanol pre-treatment improves vegetable drying and rehydration: Kinetics, mechanisms and impact on viscoelastic properties. *Journal of Food Engineering, 233*, 17–27. https://doi.org/10.1016/j.jfoodeng.2018.03.028

Rojas, M. L., & Augusto, P. E. D. (2018c). Microstructure elements affect the mass transfer in foods: The case of convective drying and rehydration of pumpkin. *LWT, 93*, 102–108. https://doi.org/10.1016/j.lwt.2018.03.031

Rojas, M. L., Augusto, P. E. D., & Cárcel, J. A. (2020). Ethanol pre-treatment to ultrasound-assisted convective drying of apple. *Innovative Food Science & Emerging Technologies, 61*, Article 102328. https://doi.org/10.1016/j.ifset.2020.102328

Rojas, M. L., Silveira, I., & Augusto, P. E. D. (2019). Improving the infrared drying and rehydration of potato slices using simple approaches: Perforations and ethanol. *Journal of Food Process Engineering, 42*(5), 13081–13089. https://doi.org/10.1111/jfpe.13089

Sakooei-Vayghan, R., Peighambardoust, S. H., Hesari, J., & Peressini, D. (2020). Effects of osmotic dehydration (with and without sonication) and pectin-based coating pretreatments on functional properties and color of hot-air dried apricot cubes. *Food Chemistry, 311*, Article 125978. https://doi.org/10.1016/j.foodchem.2019.125978

Santos, K. C., Guedes, J. S., Rojas, M. L., Carvalho, G. R., & Augusto, P. E. D. (2021). Enhancing carrot convective drying by combining ethanol and ultrasound as pre-treatments: Effect on product structure, quality, energy consumption, drying and rehydration kinetics. *Ultrasonics Sonochemistry, 70*, Article 105304. https://doi.org/10.1016/j.ultsonch.2020.105304

Scott, W. J. (1957). *Water Relations of Food Spoilage Microorganisms*, in Adv. Food Res., vol. III, Academic Press, New York.

Shen, Q., Wang, M., Tian, J., Hu, L., Ren, S., Chen, J., Ye, X., & Liu, D. (2018). Effects of Chinese pickled and dried mustard on nutritional quality, sensory quality, and shelf life of steamed pork belly. *Food Science & Nutrition, 6*, 747–756. https://doi.org/10.1002/fsn3.612

Shi, Y., Chen, G., Chen, K., Chen, X., Hong, Q., & Kan, J. (2021). Assessment of fresh star anise (Illicium verum Hook.f.) drying methods for influencing drying characteristics, color, flavor, volatile oil and shikimic acid. *Food Chemistry, 342*, Article 128359. https://doi.org/10.1016/j.foodchem.2020.128359

Solomon, W. K., & Jindal, V. K. (2017). Application of Peleg's equation to describe creep responses of potatoes under constant and variable storage conditions. *Journal of Texture Studies, 48*(3), 193–197. https://doi.org/10.1111/jtxs.12239

Su, X., Wang, B. X., Jiao, X., Zhang, C., Wen, L. K., He, Y. (2022). Component Screening and Characterization of Auricularia auricula Polysaccharide Based on Improving Rehydration Characteristics of Dehydrated Turnip. *Food Science*. http://kns.cnki.net/kcms/detail/11.2206.TS.20220309.2021.018.html. [Translate in Chinese].

Tan, S., Ke, Z., Chai, D., Miao, Y., Luo, K., & Li, W. (2021). Lycopene, polyphenols and antioxidant activities of three characteristic tomato cultivars subjected to two drying methods. *Food Chemistry, 338*, Article 128062. https://doi.org/10.1016/j.foodchem.2020.128062

Tao, Y., Han, M., Gao, X., Han, Y., Show, P. L., Liu, C., Ye, X., & Xie, G. (2019). Applications of water blanching, surface contacting ultrasound-assisted air drying, and their combination for dehydration of white cabbage: Drying mechanism, bioactive profile, color and rehydration property. *Ultrasonics Sonochemistry, 53*, 192–201. https://doi.org/10.1016/j.ultsonch.2019.01.003

Tepe, T., & Tepe, F. (2020). The comparison of drying and rehydration characteristics of intermittent-microwave and hot-air dried-apple slices. *Heat and Mass Transfer, 56*. https://doi.org/10.1007/s00231-020-02907-9

Thomson, T. L., Peart, P. M., & Foster, G. H. (1968). Mathematical simulation of corn drying a new model. *Transactions of the ASAE*, *11*(4), 582–586. https://doi.org/10.13031/2013.39473.

Uribe, E., Vega-Gálvez, A., Di Scala, K., Oyanadel, R., Saavedra Torrico, J., & Miranda, M. (2011). Characteristics of Convective Drying of Pepino Fruit (Solanum muricatum Ait.): Application of Weibull Distribution. *Food and Bioprocess Technology, 4*(8), 1349–1356. https://doi.org/10.1007/s11947-009-0230-y

Wang, B. X., Li, Y., Lv, Y. C., Jiao, X., Wang, Z. T., He, Y., & Wen, L. K. (2023). Dehydration–rehydration mechanism of vegetables at the cell-wall and cell-membrane levels and future research challenges. *Critical Reviews in Food Science and Nutrition*. https://doi.org/10.1080/10408398.2023.2233620

Wang, H., Fang, X.-M., Sutar, P. P., Meng, J.-S., Wang, J., Yu, X.-L., & Xiao, H.-W. (2021). Effects of vacuum-steam pulsed blanching on drying kinetics, colour, phytochemical contents, antioxidant capacity of carrot and the mechanism of carrot quality changes revealed by texture, microstructure and ultrastructure. *Food Chemistry, 338*, Article 127799. https://doi.org/10.1016/j.foodchem.2020.127799

Wang, J., Fang, X. M., Mujumdar, A. S., Qian, J. Y., Zhang, Q., Yang, X. H., Liu Y. H., H., Gao, Z. J., Xiao, H. W. (2017). Effect of high-humidity hot air impingement blanching (HHAIB) on drying and quality of red pepper (Capsicum annuum L.). *Food Chemistry*, *220*, 145–152. https://doi.org/10.1016/j.foodchem.2016.09.200.

Wang, J., Mujumdar, A. S., Deng, L.-Z., Gao, Z.-J., Xiao, H.-W., & Raghavan, G. S. V. (2018). High-humidity hot air impingement blanching alters texture, cell-wall polysaccharides, water status and distribution of seedless grape. *Carbohydrate Polymers, 194*, 9–17. https://doi.org/10.1016/j.carbpol.2018.04.023

Wang, J., Pei, Y.-P., Chen, C., Yang, X. H., An, K., & Xiao, H. W. (2023). High-humidity hot air impingement blanching (HHAIB) enhances drying behavior of red pepper via altering cellular structure, pectin profile and water state. *Innovative Food Science & Emerging Technologies, 83*, Article 103246. https://doi.org/10.1016/j.ifset.2022.103246

Wang, L., Xu, B., Wei, B., & Zeng, R. (2018). Low frequency ultrasound pretreatment of carrot slices: Effect on the moisture migration and quality attributes by intermediate-wave infrared radiation drying. *Ultrasonics Sonochemistry, 40*, 619–628. https://doi.org/10.1016/j.ultsonch.2017.08.005

Wang, X., Feng, Y., Zhou, C., Sun, Y., Wu, B., Yagoub, A. E. A., & Aboagarib, E. A. A. (2019). Effect of vacuum and ethanol pretreatment on infrared-hot air drying of scallion (Allium fistulosum). *Food Chemistry, 295*, 432–440. https://doi.org/10.1016/j.foodchem.2019.05.145

Warner, D. T. (1962). Nature. *Lond., 196*, 1055.

Wei, Q., Huang, J., Zhang, Z., Lia, D., Liu, C., Xiao, Y., Lagnika, C., & Zhang, M. (2019). Effects of different combined drying methods on drying uniformity and quality of dried taro slices. *Drying Technology, 37*(3), 322–330. https://doi.org/10.1080/07373937.2018.1445639

Xu, L., Fang, X., Wu, W., Chen, H., Mu, H., & Gao, H. (2019). Effects of high-temperature pre-drying on the quality of air-dried shiitake mushrooms (Lentinula edodes). *FoodChemistry, 285*, 406–413. https://doi.org/10.1016/j.foodchem.2019.01.179

Xu, W., Song, C., Li, Z., Song, F., Hu, S., Li, J., Zhu, G. Y., & Vijaya Raghavan, G. S. (2018). Temperature gradient control during microwave combined with hot air drying. *Biosystems Engineering, 169*, 175–187. https://doi.org/10.1016/j.biosystemseng.2018.02.013

Xu, Y., Xiao, Y., Lagnika, C., Li, D., Liu, C., Jiang, N., Song, J. F. Zhang, M. (2020). A comparative evaluation of nutritional properties, antioxidant capacity and physical characteristics of cabbage (Brassica oleracea var. Capitate var L.) subjected to different drying methods. *Food Chemistry*, *309*, 124935. https://doi.org/10.1016/j.foodchem.2019.06.002.

Zdunek, A., Pieczywek, P. M., & Cybulska, J. (2021). The primary, secondary, and structures of higher levels of pectin polysaccharides. *Comprehensive Reviews in Food Science and Food Safety, 20*(1), 1101–1117. https://doi.org/10.1111/1541-4337.12689

Zhang, L., Qiao, Y., Wang, C., Liao, L., Shi, D., An, K., & Shi, L. (2020). Influence of high hydrostatic pressure pretreatment on properties of vacuum-freeze dried strawberry slices. *Food Chemistry, 331*, Article 127203. https://doi.org/10.1016/j.foodchem.2020.127203

Zhang, X. L., Zhong, C. S., Mujumdar, A. S., Yang, X. H., Deng, L. Z., Wang, J., & Xiao, H. W. (2019). Cold plasma pretreatment enhances drying kinetics and quality attributes of chili pepper (Capsicum annuum L.). *Journal of Food Engineering, 241*, 51–57. https://doi.org/10.1016/j.jfoodeng.2018.08.002

Zhao, Y., Bi, J., Yi, J., Njoroge, D. M., Peng, J., & Hou, C. (2019). Comparison of dynamic water distribution and microstructure formation of shiitake mushrooms during hot air and far infrared radiation drying by low-field nuclear magnetic resonance and scanning electron microscopy. *Journal of the Science of Food and Agriculture, 99*(6), 2826–2834. https://doi.org/10.1002/jsfa.9494

Zhao, Y., Zhu, H., Xu, J., Zhuang, W., Zheng, B., Lo, Y. M., . . . Tian, Y. (2021). Microwave vacuum drying of lotus (Nelumbo nucifera Gaertn.) seeds: Effects of ultrasonic pretreatment on color, antioxidant activity, and rehydration capacity. *LWT*, *149*, 111603. https://doi.org/10.1016/j.lwt.2021.111603.

Zhou, C., Feng, Y., Zhang, L., Yagoub, A. E. A., Wahia, H., Ma, H., … Yu, X. (2021). Rehydration characteristics of vacuum freeze- and hot air-dried garlic slices. *LWT, 143*, Article 111158. https://doi.org/10.1016/j.lwt.2021.111158

Zhou, Y. H., Sutar, P. P., Vidyarthi, S. K., Zhang, W. P., Yu, X. L., Li, X. Y., … Xiao, H. W. (2022). High-humidity hot air impingement blanching (HHAIB): An emerging technology for tomato peeling. *Innovative Food Science & Emerging Technologies, 77*, Article 102987. https://doi.org/10.1016/j.ifset.2022.102987

Zhou, Y. H., Vidyarthi, S. K., Zhong, C. S., Zheng, Z. A., An, Y., Wang, J., Wei, Q., & Xiao, H. W. (2020). Cold plasma enhances drying and color, rehydration ratio and polyphenols of wolfberry via microstructure and ultrastructure alteration. *LWT, 134*, Article 110173. https://doi.org/10.1016/j.lwt.2020.110173

Zura-Bravo, L., Ah-Hen, K., Vega-Gálvez, A., García-Segovia, P., & Lemus-Mondaca, R. (2013). Effect of Rehydration Temperature on Functional Properties, Antioxidant Capacity and Structural Characteristics of Apple (Granny Smith) Slices in Relation to Mass Transfer Kinetics. *Journal of Food Process Engineering, 36*(5), 559–571. https://doi.org/10.1111/jfpe.12018